scientific reports

Check for updates

OPEN

A repurposing Dapagliflozin via polymeric nanogels for colorectal cancer therapy

Samaa Abdullah[1,6,7]✉, Samar Thiab[1,7], Abeer A. Altamimi[2], Alaa A. Al-Masud[3], Sarah Fahmi Faludah[3] & Ahmed Saud Abdulhameed[4,5]

Dapagliflozin (DAPA), a selective SGLT2 inhibitor approved for type 2 diabetes, shows emerging potential for repurposing in oncology due to its anti-inflammatory and antiproliferative properties. However, its poor solubility and rapid systemic clearance limit its therapeutic utility in cancer treatment. Here, we report the development of an oral novel gravity-induced nano hydrogel mass system encapsulating DAPA using sodium alginate (SA) and polyvinyl alcohol (PVA) nanoparticles (DAPA-PVA-SA-NPs). The formulation exhibited enhanced solubility (1.8-fold increase), high encapsulation efficiency (88.37%), and sustained release in simulated gastrointestinal conditions. In vitro studies demonstrated improved cytotoxicity against HCT-116 colorectal cancer cells and significant downregulation of oncogenic and inflammatory markers (KRAS, IL-6, TGF-β, TNF-α). In vivo pharmacokinetic evaluation in rats showed delayed Tmax, extended half-life, and a 7% increase in AUC, indicating prolonged systemic exposure with modest AUC improvement. This delivery platform improves oral exposure in rats, shows in vitro activity in HCT-116 cells and supporting further exploratory evaluation for repurposing DAPA in colorectal cancer, pending confirmation in additional models.

Keywords Dapagliflozin, Polymeric nanogels, Drug repurposing, Colorectal cancer, Oral drug delivery system, In vivo absorption

Colorectal cancer (CRC) remains a major global health burden, ranking among the leading causes of cancer-related mortality worldwide. The aggressive nature of the disease, characterized by rapid progression and high recurrence, underscores the urgent need for novel therapeutic strategies or the repurposing of existing drugs to enhance treatment efficacy and improve patient outcomes[1]. Among emerging candidates for drug repositioning is Dapagliflozin (DAPA), a selective sodium-glucose co-transporter 2 (SGLT2) inhibitor primarily used in the management of type 2 diabetes mellitus. By reducing glucose reabsorption in the renal proximal tubules, DAPA not only lowers blood glucose levels but also demonstrates pharmacological versatility that may be extended to oncology[2,3]. In recent years, the repurposing of SGLT2 inhibitors such as DAPA has emerged as a promising avenue in oncology, particularly due to their effects on glucose metabolism, oxidative stress, and inflammation pathways involved in tumour progression[4,5]. However, a key limitation in clinical translation lies in the inadequate site-specific delivery and systemic bioavailability of DAPA when administered orally. This study aims to bridge this translational gap by employing a pH-responsive sediment-forming polymeric nanogel system that potentially prolongs gastric residence time and enables a controlled release profile favourable for colonic exposure. Unlike existing DAPA-loaded bilosomes, solid lipid nanoparticles (SLNs), or self-nanoemulsifying drug delivery systems (SNEDDS), which have demonstrated systemic absorption improvements[6,7], our formulation uniquely targets the distal gastrointestinal tract via a sedimentation-mediated gel matrix. This distinction is of therapeutic importance given that CRC progression is heavily influenced by localized bioavailability and sustained drug exposure within the colonic region.

[1]Faculty of Pharmacy, Applied Science Private University, Amman 11937, Jordan. [2]Natural and Health Sciences Research Centre, Princess Nourah Bint Abdulrahman University, P.O. Box 84428, 11671 Riyadh, Saudi Arabia. [3]Tissue Banking Section, Research department, Health Science Research Center, Princess Nourah Bint Abdulrahman University, 84428 Riyadh, Saudi Arabia. [4]Department of Pharmaceutical Chemistry, College of Pharmacy, University of Anbar, Ramadi, Iraq. [5]College of Engineering, University of Warith Al-Anbiyaa, Karbala, Iraq. [6]Innovative NanoBioTech & Translational Drug Delivery Research Group, Faculty of Pharmacy, Applied Science Private University, 11937 Amman, Jordan. [7]Samaa Abdullah and Samar Thiab Authors are equally contributed. ✉email: abdullahtsamaa@gmail.com

Recent evidence has highlighted DAPA's pleiotropic actions, including modulation of oxidative stress, AMP-activated protein kinase (AMPK) signalling, and pro-inflammatory pathways such as NF-κB and TNF-α, all of which play crucial roles in tumour initiation and progression[8–10]. Moreover, DAPA has been reported to attenuate cellular markers associated with cancer cell proliferation and metastasis, such as MMPs, Ki-67, and VEGF, further supporting its potential utility in targeting solid tumours[3,11–13].

In colorectal cancer specifically, the molecular pathogenesis is intricately linked to aberrant activation of oncogenes (e.g., KRAS, BRAF, and MYC) and loss of function of tumour suppressor genes (e.g., APC, TP53, and SMAD4). Mutations in these genes dysregulate critical pathways such as MAPK, Wnt/β-catenin, and TGF-β, promoting uncontrolled proliferation, resistance to apoptosis, and enhanced metastatic potential[14,15]. Given DAPA's ability to interfere with several of these signalling pathways, its repurpose offers an attractive avenue for colorectal cancer therapy, particularly when combined with advanced delivery systems that overcome its inherent pharmacokinetic limitations.

One of the primary barriers to DAPA's clinical application in oncology is its poor aqueous solubility and rapid systemic elimination, which result in low bioavailability and suboptimal therapeutic targeting. To address these challenges, the present study aimed to formulate an oral long-acting gravity-induced hydrogel mass encapsulating DAPA in a nanoparticulate matrix. This approach leverages the synergistic properties of sodium alginate (SA), a pH-responsive biopolymer, and polyvinyl alcohol (PVA), a hydrophilic film-forming agent, to produce DAPA-loaded SA-PVA nanoparticles (DAPA-PVA-SA-NPs) that can transform into gravity-induced hydrogel mass under gastric conditions.

The rationale for selecting SA and PVA stems from their biocompatibility, mucoadhesiveness, and structural properties that enable sustained release and gravity-induced sustained-release system for oral delivery. SA, composed of mannuronic and guluronic acid residues, forms ionic crosslinked gels in acidic environments, a property advantageous for targeting the colonic region. PVA, with its capacity for hydrogen bonding and film formation, enhances nanoparticle stabilization and drug[16,17]. Together, these polymers were employed to create a hybrid nanogel system capable of overcoming physiological barriers in the gastrointestinal tract. The studied sediment-forming polymeric nanogel system is optimized to settle in the gastric fluid, forming a dense network that extends retention and facilitates pH-responsive drug release. This strategy diverges from both immediate-release systems and conventional mucoadhesive formulations by exploiting gravity-induced sedimentation, which is rarely utilized for oral delivery platforms. The biological rationale for this approach is that prolonged gastric retention and delayed release may improve drug presence in the distal gut, which is crucial for targeting inflammation and tumour pathways in colorectal cancer.

Nanoparticles between 50 and 300 nm are well-recognized for enhancing solubility, cellular uptake, and tissue penetration. In this study, nanoprecipitation and high-shear sonication methods were used to optimize the DAPA-PVA-SA-NPs, followed by their incorporation into gravity-induced hydrogel mass using high molecular weight SA solutions. Comprehensive physicochemical characterizations, including Fourier Transform Infrared Spectroscopy (FT-IR), Powder X-ray Diffraction (PXRD), Scanning Electron Microscopy (SEM), and Transmission Electron Microscopy (TEM), were employed to validate successful encapsulation, assess morphological properties, and elucidate drug-polymer interactions.

To evaluate the formulation's therapeutic potential, in vitro solubility, drug release, and sedimentation analyses were performed, complemented by cytotoxicity assays against HCT-116 colorectal cancer cells and ELISA-based quantification of oncogenic and inflammatory markers. Furthermore, in vivo pharmacokinetic studies were conducted in Wistar rats to compare the plasma profiles of free DAPA suspension versus the optimized gravity-induced nanohydrogel mass formulation.

In summary, this study introduces a novel gravity-induced hydrogel mass forming nanoparticulate delivery system for Dapagliflozin with the dual objectives of enhancing its solubility and achieving desired colorectal delivery. By improving pharmacokinetic properties and modulating key oncogenic pathways, the DAPA-PVA-SA nanogel system represents a promising therapeutic strategy for repurposing DAPA in colorectal cancer treatment.

Materials and methods

Materials

DAPA was generously provided by Sigma-Aldrich, USA. SA, a biocompatible polymer with a low molecular weight grade (5,000–20,000 Da), was purchased from Sigma-Aldrich, USA. PVA, used as a stabilizing and film-forming agent in the nanoparticle formulation, was obtained from TCI America, USA.

The human colorectal cancer cell line HCT-116 was purchased from the American Type Culture Collection (ATCC, Manassas, VA, USA). To support cell culture, Dulbecco's Modified Eagle Medium (DMEM), supplemented with 10% fetal bovine serum (FBS), penicillin, and streptomycin, was sourced from Gibco, London, UK.

These materials were used to formulate and characterize the DAPA-loaded SA-PVA nanoparticles (DAPA-ALG-PVA-NPs) for developing the gravity-induced nanohydrogel mass aimed for colorectal cancer therapy.

Preparation and optimization of DAPA-ALG-PVA-NPs

To develop the optimum DAPA-ALG-PVA-NPs (Table 1), a stock solution of 30 mg/mL SA (low molecular weight grade; 5,000–20,000 Da, CAS. NO. 9005–32-7) was prepared in distilled water[16]. DAPA was dissolved in water and mixed with varying amounts of PVA (6,000 g/mol, CAS. NO. 9002–89-5) to form a 5 mL dispersion using a magnetic stirrer. This mixture aimed to enhance the stability and solubility of DAPA by forming a gravity-induced hydrogel mass suitable for colorectal cancer therapy[17–22].

To achieve homogeneous nanoparticle dispersion, the colloidal mixture of DAPA and PVA was combined with 4 mL of the prepared SA stock solution based on the method of in-house optimization. An accurately

Preparation No	PVA Concentration (mg/mL)	SA Equivalent Amount (mg/mL)	PVA: SA Ratio @	Total Volume (mL)	Particle Size (nm)*	PDI*
1	5	15	1:3	10	500.50 ± 18.90	0.83 ± 0.07
2	10		1:2		90.40 ± 20.90	0.32 ± 0.03
3	15		1:1		305.71 ± 10.82	0.53 ± 0.11

Table 1. Optimization of DAPA-PVA-SA-NPs' Preparations[#]. *For n = 3, values are presented as mean ± standard deviation (SD); @ Approximate ratio with SA-Low molecular weight; DAPA concentration is 13 mg/mL.

weighed quantity of PVA was dissolved in 10 mL of distilled water, and the mixture was stirred while 2 mL of absolute ethanol was added dropwise. This mixture was then subjected to high-shear sonication using ultrasound nanomaterial dispersion equipment (Biosafer ultrasonicator, China) with a 20 kHz frequency, 2,000 W power, and a 20 mm probe diameter for 15 min. Sonication is crucial for breaking down larger aggregates and ensuring uniform distribution of DAPA within the polymeric matrix, thereby forming stable gravity-induced nanohydrogel mass[23].

The particle size and zeta potential of the resulting DAPA-PVA-SA-NP different combinations were measured using a zeta-sizer (Malvern Zeta-sizer Nano ZS, Malvern Instruments Ltd., UK). The optimized nanoparticle system was selected based on achieving the smallest particle size with a homogeneous Polydispersity Index (PDI). The zeta potential value of the most stable formulation was determined to ensure adequate surface charge for colloidal stability, as a high zeta potential indicates reduced particle aggregation and enhanced stability[24].

To isolate the drug nanoparticles from the polymeric matrix, 2 mL of the optimized nanoparticle suspension was diluted with 2 mL of distilled water and vortexed for 30 s. The mixture was then centrifuged at 3,000 rpm for 15 min to facilitate sedimentation of larger particles. The supernatant was carefully collected and analyzed to measure particle size and zeta potential, confirming the formation of a stable gravity-induced hydrogel mass system[25].

The encapsulation efficiency of DAPA within the nanoparticles was determined using UV–visible spectrophotometry (Shimadzu, Japan) by scanning the collected supernatant at 224 nm. The encapsulation efficiency was calculated using the following formula:

$$\mathrm{EncapsulationEfficiency}\,(\%) = (\mathrm{TotalDAPA} - \mathrm{FreeDAPA})/\mathrm{TotalDAPA} \times 100$$

This method ensures the accurate quantification of the encapsulated drug, providing insight into the efficiency of the gravity-induced hydrogel mass-forming system for enhanced colorectal cancer therapy[1,9].

Characterizations of optimum DAPA-ALG-PVA-NPs

Fourier transform-infrared (FT-IR)

Fourier-Transform Infrared (FT-IR) spectroscopy analysis was conducted to characterize the chemical interactions, and functional groups present in the samples. The analysis included DAPA, PVA, SA, the physical mixture, blank PVA-SA-NPs, and the optimum DAPA-PVA-SA-NPs (10 mg). The FT-IR spectra were recorded using a Thermo-Scientific Nicolet iS10 FT-IR spectrometer (USA). The samples were scanned over a wavenumber range of 500 to 4,000 cm^{-1} with high resolution to accurately capture the characteristic peaks and interactions between the components[16].

Powder X-ray diffractometer (PXRD)

Powder X-ray diffraction (PXRD) analysis was performed to investigate the crystalline structure and phase composition of the samples, including DAPA, PVA, SA, the physical mixture, blank PVA-SA-NPs, and the optimum DAPA-PVA-SA-NPs. The analysis was conducted using a Maxima XRD-7000X powder X-ray diffraction system (Rigaku, Ultima IV XRD, Japan). During the measurement, X-rays were produced at a voltage of 40 kV and a current of 40 mA, utilizing a nickel-filtered Cu-Kβ radiation source. The diffraction patterns were recorded over a 2θ scan range of 5 to 70 degrees at a scanning speed of 10 degrees per minute, ensuring detailed crystalline structure analysis[23].

Morphology and dispersion investigations

SEM analysis was performed to study the surface morphology and particle distribution of DAPA, PVA, SA, the physical mixture, blank PVA-SA-NPs, and the optimum DAPA-PVA-SA-NPs in their powder form. The samples were analyzed using a JSM-7600F SEM system (Jeol, Japan), operating at a voltage of 30 kV. This technique provided high-resolution images to observe surface characteristics and particle size distribution, confirming the successful formation of nanoparticles[26–28].

TEM was used to investigate the internal morphology and size of the optimum DAPA-PVA-SA-NPs. The analysis was conducted using a JEM-F200 TEM system (Jeol, Japan). The samples were negatively stained with 2% phosphotungstic acid, and one drop of the appropriately diluted suspension was placed on a copper grid[17].

Solubility assessment

Samples of DAPA and the optimum DAPA-PVA-SA-NPs containing more than 10 mL of the test fluid were placed in 15 mL centrifuge tubes. The samples were thoroughly mixed using a vortex mixer for 15 min to ensure

homogeneity. Subsequently, the tubes were placed in a shaking water bath and incubated for 72 h to facilitate thorough mixing and equilibration.

After incubation, the samples were centrifuged to separate the supernatant. The collected supernatant was then dissolved in a measured volume of ethanol for analysis. The DAPA content was quantified using UV-spectrophotometry at the λmax of 224 nm, which is the characteristic absorption maximum for Dapagliflozin, allowing accurate determination of drug concentration[29].

Formulation and optimization of sediment-forming gel encapsulating DAPA-PVA-SA-NPs

The optimized DAPA-PVA-SA-NPs formulation (Table 2), containing 13 mg/mL DAPA, was prepared by suspending the nanoparticles in varying volumes of SA-high molecular weight (600,000 g/mol) using a 3% stock solution. The suspension process was carried out using a stirrer machine for 10 min to ensure uniform distribution and consistency of the sediment-forming gel[18,19].

DAPA release analysis

The release of DAPA was evaluated using three sediment-forming gel formulations (F1-F3), the raw DAPA material, and the optimized DAPA-loaded co-polymeric nanoparticles (DAPA-PVA-SA-NPs). The analysis was performed at a controlled temperature of 37.00 ± 0.05 °C in a shaker set to 75.00 ± 0.05 rpm. The raw DAPA material was dispersed in distilled water to achieve a concentration of 13 mg/mL, similar to the optimized DAPA-PVA-SA-NPs formulation[23].

The samples were placed in dialysis bags with a molecular weight cut-off range of 12,000–14,000 (Sigma, USA), which were then immersed in 300 mL of release medium. Initially, for the first two hours, the samples were immersed in 0.1N HCl, representing simulated stomach fluid with a pH of 1.2. Subsequently, the dialysis bags were transferred to a phosphate buffer with a pH of 6.8, mimicking the proximal intestinal fluid environment. To maintain sink conditions, the medium was completely replaced every hour during the experiment[30].

This dual-phase release method, involving both acidic and neutral conditions, was designed to simulate the gastrointestinal transit of the DAPA-loaded formulations, ensuring the assessment of release kinetics in both stomach and intestinal environments[29].

Sediment characterization analysis

The sediment-forming gels described in Table 2 were characterized by evaluating their strength, volume, and resilience. These characterization parameters, along with release profiles, served as key selection criteria for determining the optimal sediment-forming gel encapsulating DAPA-loaded co-polymeric nanoparticles (DAPA-PVA-SA-NPs)[18,19]. The properties measured included the volume, weight, strength, and resilience of the sediment formed in 0.1N HCl, mimicking the stomach environment.

Sediment gel density

Sediment gel was assessed using a 250 mL glass beaker, which was pre-weighed to obtain the initial weight (W1). A volume of 15 mL of the gel formulation was added to 150 mL of 0.1N HCl. After the insoluble sediment gel was formed (approximately 30 min), the bottom position of the gravity-induced hydrogel mass was marked on the beaker. The total weight of the beaker and contents (W2) was recorded. After gently decanting the supernatant liquid, the insoluble gel was carefully removed and placed on a pre-tared watch glass. The supernatant was drained after 30 s, and the insoluble gel was weighed (W3). The remaining liquid was wiped off with a paper towel, and the beaker was refilled with water up to the marked level and then weighed again (W4).

The insoluble gel volume (mL) was calculated using the formula:

$$\text{Insoluble GelVolume} = (W4 - W1) - (W2 - W1 - W3)$$

This calculation assumes a supernatant density of 1 g/mL, which is typical for aqueous solutions[31].

Sediment gel durability

To evaluate insoluble gel durability, 15 mL of each gel formulation was mixed with 150 mL of 0.1N HCl and kept at 37 °C in a 50 mL centrifuge tube. The tube was sealed and subjected to gentle agitation at 20 rpm using a Roller Mixer-205 RM (Hawashin Tech. Company, Korea), simulating stomach movement. The insoluble was visually inspected at intervals of 2, 5, 10, 20, 30, 45, and 120 min, or until it either gravity-induced hydrogel mass or became invisible. The sediment gel's durability was defined as the time taken for the insoluble gravity-induced hydrogel mass to completely disintegrate or disappear[24].

#	SA*-gel (mg/mL)	PVA : SA**	DAPA (mg/mL)
F1	6	1.67: 1	13
F2	12	1: 1.2	
F3	18	1: 1.8	

Table 2. Sediment-forming gels components encapsulating DAPA-PVA-SA-NPs'. *SA: High molecular weight (600,000 g/mol); **PVA: Low molecular weight (10,000 g/mol).

Sediment gel strength

The insoluble gel's strength was measured using a Texture Analyzer XT Plus C (Stable Micro Systems, UK). Insoluble gels were created by adding 15 mL of the formulation to 150 mL of 0.1N HCl at 37 °C and allowing them to form over 30 min in a 250 mL glass beaker. The formed sediments were removed, and the force required to break the insoluble gel using a stainless-steel cone was measured. The force (N) was calculated as:

$$\text{Insoluble Sediment Strength} = \text{Force}\,(\text{Kg}\cdot\text{m/s})\,/\text{Acceleration}\,(\text{m/s})$$

The result was expressed as mass (g), indicating the gravity-induced hydrogel mass's mechanical integrity and stability[30].

Cell viability assay

The therapeutic efficacy of the optimum DAPA-loaded nanoparticles (DAPA-PVA-SA-NPs) was evaluated for their anti-cancer activity against colorectal cancer cell lines (HCT-116) using the MTT assay. This assay was conducted to assess cell viability following the release of nanoparticles from the gravity-induced hydrogel mass[18].

HCT-116 colorectal carcinoma cells were obtained from ATCC and authenticated using short tandem repeat (STR) profiling, with mycoplasma contamination testing performed within 6 months prior to experimentation. Cells were seeded in 96-well plates (1×10^4 cells/well) and treated with increasing concentrations (1–100 µg/mL) for 24 h in complete medium (DMEM with 10% FBS, 1% penicillin/streptomycin). Dose–response curves were generated using GraphPad Prism (v9.0), fitted to a four-parameter logistic regression model. Results are expressed as mean ± SD from three biological and three technical replicates per dose, with 50%-inhibitory concentration (IC50) reported in both µg/mL and µM, including 95% confidence intervals. The experimental setup included various treatment groups of blank PVA-SA NPs, DAPA-PVA-SA-NPs, Pure DAPA, Control (untreated cancer cells) and Negative control (culture media without cells).

After the initial incubation period, the cells were treated with the selected groups and incubated for an additional 24 h under the same conditions[23].

Post-incubation, all samples from the cell plates were centrifuged, and the supernatant (100 µL) was collected and replaced with DMSO to dissolve the formazan crystals formed during the MTT assay. The samples were then returned to the CO_2 incubator at 37 °C for 4 h to complete the reaction.

After the final incubation, the absorbance of each well was measured at 570 nm using a microplate reader. Each test was performed in triplicate to ensure accuracy and reproducibility. The absorbance values were used to calculate cell viability by comparing the treated groups with the control group[24].

ELISA test

The levels of KRAS, TGF-β, IL-6, and TNF-α were quantified to assess the inflammatory, oncogenic, metastatic, and apoptotic responses associated with the treatment using the IC50 values of blank PVA-SA NPs, DAPA-PVA-SA-NPs, Pure DAPA, Control, which were extracted from the cell viability assays[32–34]. While KRAS-mutant HCT-116 cells typically exhibit constitutive KRAS expression, prior studies suggest that metabolic stress or inflammation-modulating agents may influence KRAS protein levels indirectly[35]. All data were collected under blinded conditions. These biomarkers are critically involved in colorectal cancer progression and inflammation[9]. Commercially available ELISA kits were used for quantification, including KRAS and TGF-β kits from Abcam, UK, and IL-6 and TNF-α kits from Invitrogen, USA. The assays were performed according to the manufacturer's protocols to ensure accuracy and reproducibility[23,36–39]. The absorbance readings were recorded at the specified wavelengths using a microplate reader, and the concentrations were calculated using standard curves provided with the kits[24]. This quantification approach effectively evaluated the anti-inflammatory and anti-tumorigenic potential of the DAPA-loaded nanoparticles, demonstrating its relevance for colorectal cancer treatment[29]. For biomarker analysis, cell lysates were prepared and total protein measured by BCA assay. KRAS, TGF-β, IL-6, and TNF-α levels were quantified using commercially available sandwich ELISA kits, validated for human targets. ELISA data were normalised to total protein content. Given the constitutively active KRAS mutation in HCT-116 cells, the reduction observed via ELISA may not reflect direct transcriptional or pathway-level inhibition. Additional analysis such as qPCR or ERK/MAPK signaling would be needed to confirm this.

In vivo evaluation: DAPA plasma concentration and pharmacokinetics in rats

All animal experiments were approved by the Institutional Animal Care and Use Committee (IACUC) of Princess Nourah bint Abdulrahman University, Saudi Arabia (Approval Number: HA-01-R-104). All procedures involving animals were carried out in strict accordance with the institutional guidelines of the Animal Research Ethics Committee of Princess Nourah bint Abdulrahman University and in compliance with the National Committee of Bio-Ethics (NCBE) guidelines regulated by King Abdulaziz City for Science and Technology (KACST), Saudi Arabia. Additionally, all methods are reported in accordance with the ARRIVE guidelines (https://arriveguidelines.org) for the reporting of animal experiments.

The in vivo pharmacokinetic study of the optimum DAPA-loaded gel nanoparticles (DAPA-PVA-SA-NPs) was conducted using male Wistar rats weighing 200–250 g, n = 6 for each group. The rats were housed in standard laboratory conditions with a 12-h light/dark cycle, temperature of 22 ± 2°C, and humidity of 55 ± 5%. Prior to blood collection via retro-orbital plexus, rats were anesthetized using 2–3% isoflurane inhalation in an induction chamber to minimize pain and distress. At the end of the experiment, animals were humanely euthanized via carbon dioxide (CO_2) inhalation followed by cervical dislocation, in accordance with the AVMA Guidelines for the Euthanasia of Animals (2020 edition). At the time of euthanasia via cervical dislocation, the body weight of the Wistar rats ranged between 240 and 250 g, with a mean weight of 245 ± 2.4 g[21,23].

The oral dose of DAPA was set at 10 mg/kg body weight, administered via the gel formulation or free DAPA powder suspended in water (0.76 mL). The rats were fasted for 12 h before dosing but had free access to water. The administration was performed using an oral gavage to ensure accurate delivery of the dose[9,40].

Blood samples (approximately 0.5 mL) were collected from the retro-orbital plexus at pre-determined time intervals (0, 1, 2, 4, 6, 8, 10, 12, 18, 24 and 48 h) post-administration. To prevent clotting, heparinized tubes were used. The samples were then centrifuged at 3,000 rpm for 10 min, and the plasma was separated and stored at -20°C until further analysis[24].

DAPA concentrations in rat plasma were quantified using a validated high-performance liquid chromatography (HPLC) method with ultraviolet (UV) detection at 224 nm. Chromatographic separation was achieved using a C18 reversed-phase column (150 mm × 4.6 mm, 5 µm) with a mobile phase composed of acetonitrile and phosphate buffer (pH 3.5) in a ratio of 65:35 v/v, delivered at a flow rate of 1.0 mL/minutes. The retention time of DAPA under these conditions was approximately 5.3 min, in agreement with previous reports using similar setups[41,42]. The method was validated following the bioanalytical method validation guidelines issued by the FDA (2018) and EMA (2011)[43,44]. Validation parameters included selectivity, assessed by analysing blank plasma samples from six individual rats to ensure no endogenous interference at the retention time; linearity over the concentration range of 10–2000 ng/mL, yielding an $R^2 > 0.999$; and intra- and inter-day accuracy and precision, which remained within ± 15% as per regulatory thresholds. Matrix effects and recovery were evaluated using the post-extraction spiking approach, revealing mean recoveries above 90%, and carryover was ruled out by analysing blank injections following high concentration samples. DAPA also showed stability under short-term benchtop conditions, repeated freeze–thaw cycles, and long-term storage at –80°C. Although LC–MS/MS offers higher specificity, HPLC–UV remains an acceptable and widely used approach for preclinical pharmacokinetics provided the method is fully validated[45], and this procedure offered reliable and reproducible results in the current study.

Statistical interpretation

Statistical analysis was conducted using one-way ANOVA followed by Tukey's Multiple Comparison Test to determine the significance between groups. The data were expressed as mean ± standard deviation (SD) to ensure an accurate representation of variability. A p-value ≤ 0.05 was considered statistically significant, indicating that differences between groups were unlikely to have occurred by chance. All statistical calculations were performed using GraphPad Prism 4.0 software (GraphPad Software, San Diego, USA), which is widely recognized for its robust data analysis capabilities.

Results and discussion

Selection and optimization of DAPA-PVA-SA-NPs

Three nanoparticle formulations of DAPA were developed using PVA, MW: 10,000 g/mol and SA, MW: 5,000–20,000 Da, as co-polymers, aiming to optimize particle characteristics for colorectal delivery. Each formulation maintained a constant DAPA concentration of 13 mg/mL and varied in the PVA: SA polymer ratios, as listed in Table 1.

Preparation 2 (P2) demonstrated the most promising profile with a mean particle size of 90.40 ± 20.90 nm, the lowest polydispersity index (PDI = 0.32 ± 0.03), and a moderate zeta potential of –33.22 ± 0.22 mV (**Supplementary Fig. 3, and Supplementary Fig. 4**), indicating strong colloidal stability and favourable dispersion properties. These findings are consistent with the principle that an optimal PVA-to-SA ratio enhances steric and electrostatic stabilization of polymeric nanoparticles[46,47].

In contrast, Preparation 1 (P1) showed a significantly larger particle size (500.50 ± 18.90 nm) and higher PDI (0.83 ± 0.07), despite a strongly negative zeta potential (–70 ± 0.33 mV) (**Supplementary Fig. 1, and Supplementary Fig. 2**), which likely reflects aggregation due to high polymeric entanglement or phase separation[48]. Preparation 3 (P3), while offering an intermediate size of 305.71 ± 10.82 nm, had an unstable surface charge (–5.22 ± 0.44 mV) (**Supplementary Fig. 5, and Supplementary Fig. 6**) that may compromise its dispersion and mucoadhesion efficiency[49].

Zeta potential values between –30 to –40 mV are generally accepted to offer both colloidal stability and sufficient electrostatic repulsion to prevent nanoparticle aggregation (Kazi et al., 2021). Therefore, F2's zeta potential (~ –33 mV) with an encapsulation efficiency of 88.37% ± 0.04 (**Supplementary Fig. 7 for UV-analysis)** supports its stability and mucoadhesive potential, critical for rectal retention and gravity-induced hydrogel mass behaviour in vivo.

PVA serves a dual function as a steric stabilizer and cryoprotectant, while SA acts as a pH-responsive gelling agent that enhances nanoparticle sedimentation in acidic environments such as the colon[50]. This gelation behaviour aligns with the desired gel profile for gravity-induced sustained-release system for oral delivery. These results indicate that Preparation 2 (P2) meets the critical quality attributes to be incorporated in the optimization of controlled, localized, and stable gravity-induced hydrogel mass, and is thus encapsulated in the optimized gel for subsequent in vivo and pharmacological evaluation.

Characterizations of optimum DAPA-PVA-SA-NPs

Fourier transform-infrared (FT-IR)

FT-IR spectroscopy was performed to assess potential interactions between DAPA, PVA, and SA within the optimized co-polymeric nanoparticles. The characteristic spectra of pure DAPA, individual polymers (PVA and SA), their physical mixture, blank PVA-SA nanoparticles, and DAPA-loaded PVA-SA nanoparticles (DAPA-PVA-SA-NPs) are presented in Fig. 1.

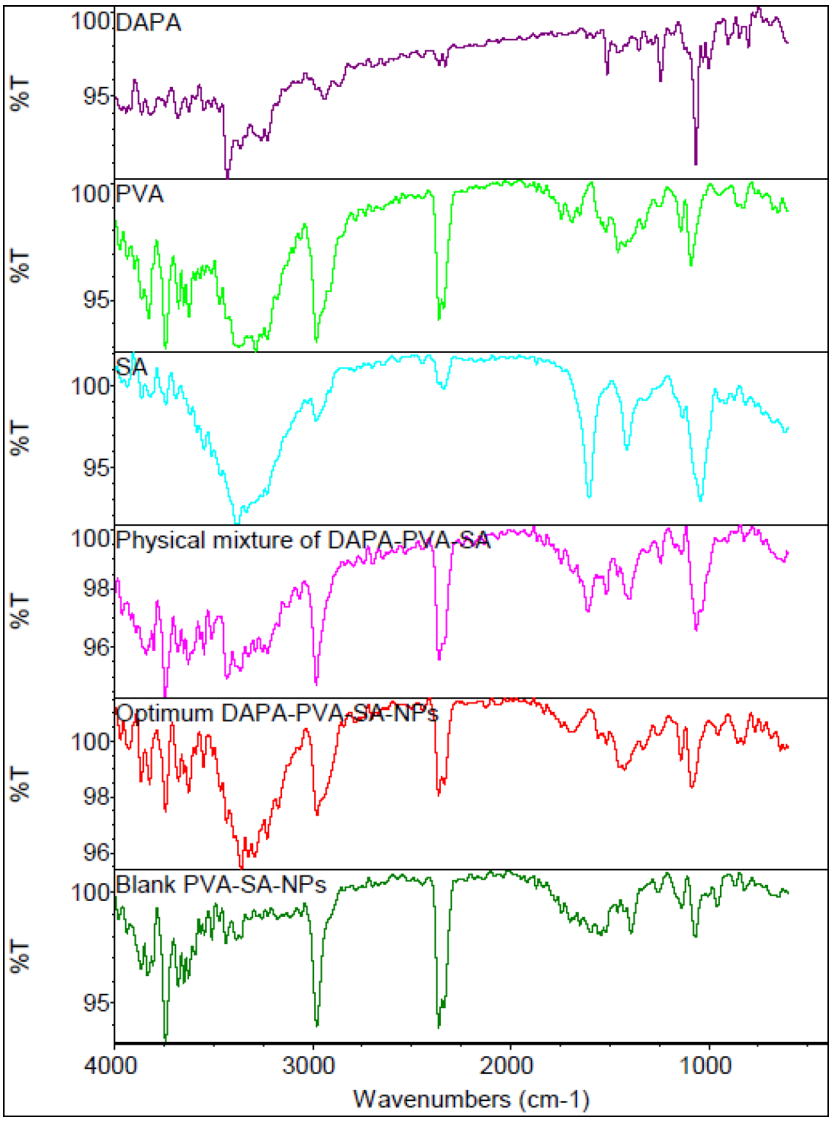

Fig. 1. FT-IR spectra of (from top to bottom): pure Dapagliflozin (DAPA), Polyvinyl Alcohol (PVA), Sodium Alginate (SA), Physical mixture of DAPA, PVA, and SA, Optimum DAPA-PVA-SA nanoparticles (DAPA-PVA-SA-NPs), and Blank PVA-SA nanoparticles. The spectra illustrate the characteristic functional group vibrations and confirm the successful encapsulation of DAPA into the co-polymeric nanoparticle matrix through observable shifts and intensity changes in the hydroxyl, carbonyl, and carboxylate regions.

The spectrum of pure DAPA showed strong and sharp peaks attributed to its functional groups: O–H stretching (~ 3371 cm^{-1}), C–H stretching (~ 2941 cm^{-1}), and prominent bands related to the C = O stretching (~ 1712 cm^{-1}) and aromatic C = C vibrations (~ 1604 and 1501 cm^{-1}), consistent with earlier reports[50,51].

The FT-IR spectrum of PVA displayed a broad band around 3300–3400 cm^{-1} due to O–H stretching, and sharp bands near 2900 cm^{-1} and 1090 cm^{-1} attributed to C–H and C–O stretching vibrations, respectively. SA exhibited characteristic bands at ~ 1600 cm^{-1} and 1415 cm^{-1}, corresponding to asymmetric and symmetric carboxylate stretching, and a peak at ~ 1030 cm^{-1} due to C–O–C vibrations in the polysaccharide backbone[47].

The physical mixture spectrum demonstrated a superimposition of individual components, with no significant shift or disappearance of peaks, indicating the absence of strong interactions at the macroscopic blend level. In contrast, the blank PVA-SA-NPs exhibited a slight broadening and reduced intensity in the hydroxyl and carboxylate regions, suggesting hydrogen bonding between polymer chains during nanoparticle formation[46].

Notably, the FTIR spectrum of DAPA-PVA-SA nanoparticles exhibited clear spectral changes, including diminished and broadened O–H and C = O peaks associated with DAPA, along with slight shifts in the carboxylate bands of SA and the hydroxyl groups of PVA, indicating successful molecular interactions. These spectral changes strongly suggest successful molecular encapsulation and hydrogen bonding between DAPA and the polymers within the nanoparticle matrix[49].

Collectively, the FT-IR analysis confirms the successful incorporation of DAPA into the PVA-SA co-polymeric matrix without chemical degradation. The observed spectral shifts and peak attenuation are indicative of strong

physical interactions and network entrapment, which may contribute to the nanoparticle stability and sustained release behaviour observed in vitro.

While previous strategies have explored enhancing DAPA's systemic bioavailability, few studies have prioritised its potential for distal intestinal exposure, a region critical for therapeutic efficacy in CRC. Bilosomes and SLNs, for example, rely predominantly on lymphatic absorption and do not leverage the pH gradients of the gastrointestinal tract[39]. Our study addresses this gap by integrating sodium alginate's acid-induced gelation properties with polyvinyl alcohol's mucoadhesive capacity, forming a gravity-induced hydrogel mass that is retained in the stomach and facilitates gradual release along the intestine. The theoretical basis of this mechanism; validated via FT-IR, sedimentation testing, and release kinetics; provides a strong rationale for colonic drug disposition, even though further in vivo imaging studies are required for confirmation.

Powder X-ray Diffractometer (PXRD)

Figure 2 shows the diffractograms for DAPA, PVA, SA, the physical mixture, blank PVA-SA nanoparticles, and the optimized DAPA-PVA-SA-NPs. The diffractogram of pure DAPA exhibited intense and sharp peaks, particularly in the 2θ range of 18° to 26°, which are indicative of its crystalline nature, aligning with previous studies that reported strong diffraction intensities for Dapagliflozin in its unmodified form[46,51].

PVA and SA, the polymeric carriers, demonstrated broad and less defined peaks, reflecting their semi-crystalline and amorphous nature, respectively[50]. The physical mixture of DAPA, PVA, and SA displayed a superimposition of the individual polymer and drug peaks, albeit with reduced intensities, suggesting a dilution of crystalline DAPA within the polymer matrix.

More notably, the diffractograms of the blank nanoparticles and DAPA-loaded PVA-SA nanoparticles (DAPA-PVA-SA-NPs) revealed significant alterations. The optimized DAPA-PVA-SA-NPs showed a markedly reduced intensity of the original DAPA peaks, replaced by broader humps characteristic of amorphous materials. This transformation from a crystalline to a partially amorphous form supports the hypothesis that DAPA was successfully encapsulated within the polymeric matrix, potentially altering its crystallinity due to the interaction with PVA and SA[47]. These structural changes are consistent with enhanced solubility and dissolution profiles observed in the nanoparticles, attributed to the increased surface area and reduced crystallinity[46,47].

The data confirms that the formulation process induced a significant shift from a crystalline to a more amorphous structure in the DAPA nanoparticles, which may contribute to improved bioavailability and therapeutic efficacy in future in vivo applications.

Morphology and dispersion investigations

The morphological characteristics and dispersion behaviours of raw materials and the fabricated DAPA-PVA-SA-NPs were assessed using Scanning Electron Microscopy (SEM), as presented in Fig. 3 **(Panels A–F)**. The SEM image of DAPA (Fig. 3A) reveals its inherent crystalline morphology, with sharp-edged and irregular coarse particles. PVA, shown in Fig. 3B, exhibits a highly agglomerated, porous surface structure consistent with semi-crystalline behaviour, whereas SA (Fig. 3C) reveals a fragmented amorphous texture, typical of polysaccharide-based biopolymers[47,51].

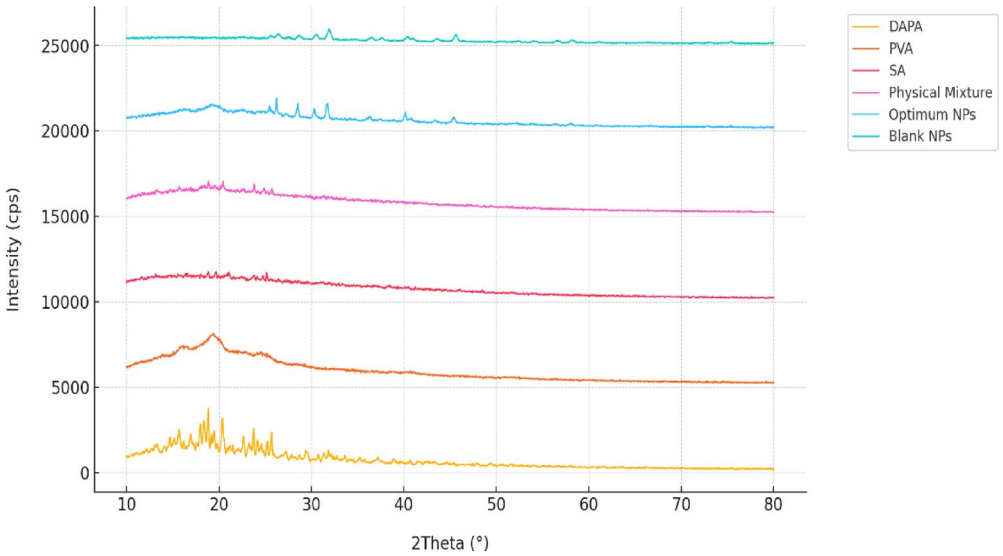

Fig. 2. Powder X-ray diffraction (PXRD) patterns of Dapagliflozin (DAPA), Polyvinyl Alcohol (PVA), Sodium Alginate (SA), physical mixture of DAPA-PVA-SA, optimum DAPA-PVA-SA nanoparticles, and blank PVA-SA nanoparticles. The sharp diffraction peaks of pure DAPA indicate its crystalline nature, while the broad patterns of polymers (PVA, SA) suggest amorphous characteristics. The disappearance of DAPA's crystalline peaks in the nanoparticle formulations confirms successful encapsulation and transformation into an amorphous form, enhancing solubility and bioavailability.

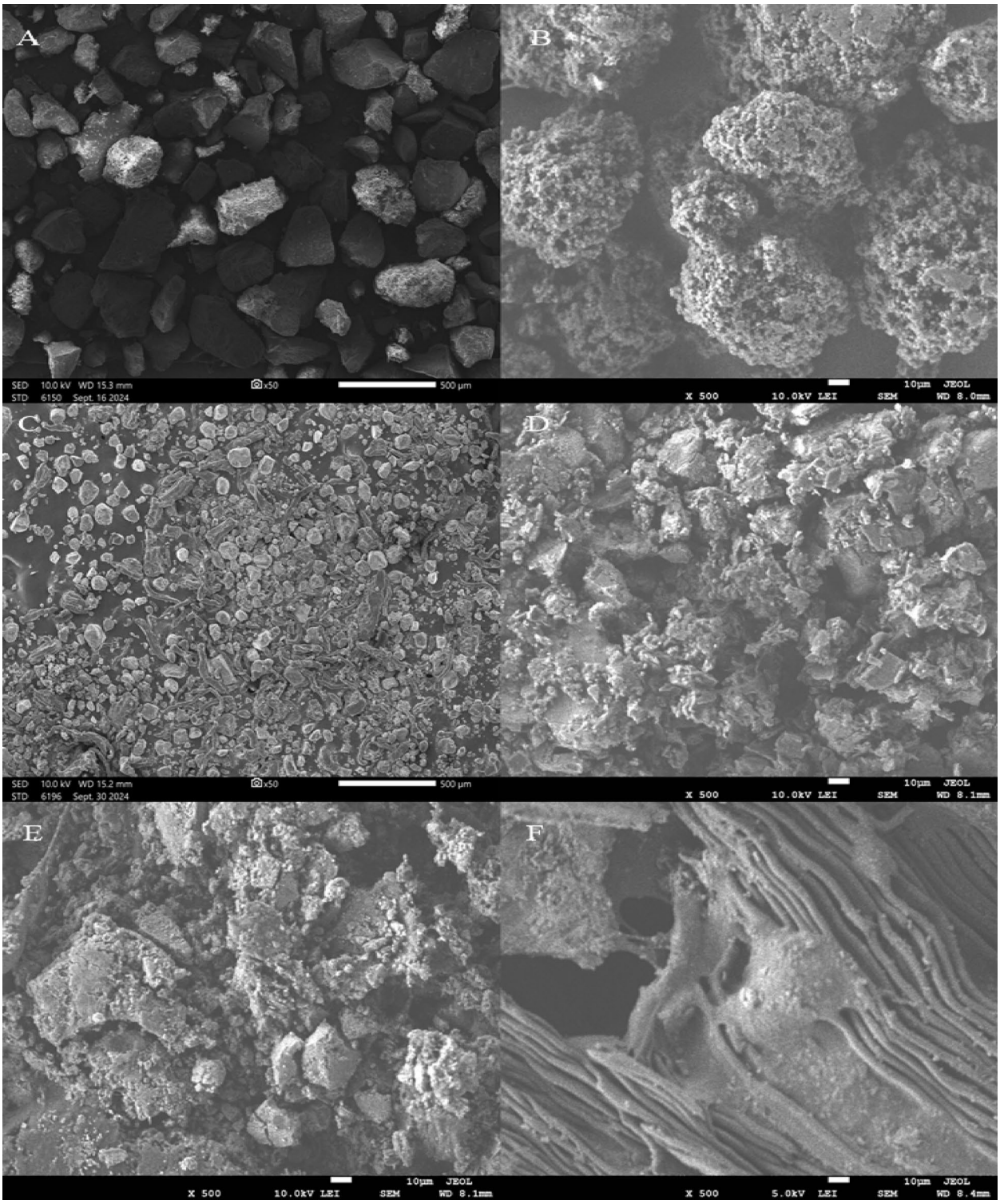

Fig. 3. Scanning Electron Microscopy (SEM) images depict the surface morphology of individual components and nanoparticle formulations. Image (A) shows pure Dapagliflozin (DAPA) as coarse, irregular crystalline particles, while (B) presents Polyvinyl Alcohol (PVA) with a porous, agglomerated texture. Sodium Alginate (SA) in (C) appears as fragmented amorphous particles. The physical mixture of DAPA, PVA, and SA in (D) reveals unevenly distributed particles with weak intermolecular binding. Image (E) illustrates blank PVA-SA nanoparticles exhibiting a rough and porous matrix structure, indicative of successful nanoparticle formation. Finally, (F) shows the optimized DAPA-PVA-SA nanoparticles with a compact, integrated surface and reduced crystallinity, confirming effective DAPA encapsulation and uniform nanoparticle morphology.

The physical mixture of DAPA, PVA, and SA (Fig. 3D) shows poorly dispersed and unevenly adhered DAPA crystals atop the polymer matrix. This dispersion suggests weak physical entrapment and minimal interaction among components, reinforcing the necessity for nanoparticulate encapsulation to improve homogeneity[46]. In contrast, the optimum DAPA-loaded PVA-SA nanoparticles (Fig. 3E) displayed a homogenous and more condensed structure, with a noticeable reduction in crystallinity and particle aggregation, indicating successful encapsulation of DAPA into the co-polymeric matrix. The consistent distribution and surface coverage imply the formation of a compact insoluble gel network structure attributed to the film-forming synergy between SA and PVA[49].

Finally, the high-magnification image of the optimized nanoparticles (Fig. 3F) showed uniform spherical particles embedded within a porous matrix. Although the monomeric units appear sub-100 nm in dimension, moderate clustering and surface roughness are observable, possibly contributing to the moderately high PDI values and sedimentation observed during formulation[52]. These SEM findings correlate well with zeta-potential data, indicating stable formulation with enhanced electrostatic repulsion and particle distribution. The (TEM) image presented here provides a high-resolution visualization of the internal morphology and size distribution of the optimum F2 of DAPA-loaded PVA-SA nanoparticles (DAPA-PVA-SA-NPs) (Fig. 3G). The nanoparticles appear as well-dispersed, nearly spherical entities with varying sizes, indicating a polydisperse system. Measurements annotated in the image show particle sizes ranging from approximately 10.64 nm to 66.39 nm, with an average size visually centred around 30–50 nm. These findings are consistent with prior reports on polymeric nanoparticle systems where a sub-100 nm size distribution is critical for cellular uptake and efficient drug delivery to cancerous tissues[49,51].

Overall, the SEM analysis confirms that the formulation of DAPA within a PVA-SA polymeric system results in nanoscale particles with superior encapsulation efficiency, altered surface morphology, and better dispersion, which are essential characteristics for improved drug release and colonic delivery applications.

The relatively uniform morphology and absence of large aggregates suggest that the high-shear sonication process employed during preparation was effective in reducing particle size and ensuring homogenous dispersion. The round-to-oval shapes of the particles are characteristic of nanostructures formed by ionic and hydrogen bonding interactions between SA and PVA, which act synergistically to form a stabilized polymeric matrix[47].

Smaller-sized particles, such as those around 10.64 nm, may exhibit faster diffusion and enhanced permeability across cellular membranes, while larger particles (~66 nm) offer advantages in sustained release and colloidal stability. The presence of such a size distribution may contribute to a biphasic release profile, supporting initial burst release followed by extended delivery, as observed in drug release studies[53].

Overall, the TEM image confirms successful nanoparticle fabrication with appropriate size, morphology, and dispersibility for colorectal cancer-targeted applications. The nanoscale size ranges not only supports efficient cellular internalization but also align with the enhanced permeability and retention (EPR) effect crucial for tumor targeting via passive mechanisms[54,55].

Solubility assessment

The solubility results presented in Table 3 show a significant enhancement in the solubility of DAPA when formulated into PVA-SA nanoparticles. In simulated gastric fluid (0.1N HCl), the solubility of DAPA-raw material was only 1.05 ± 0.02 mg/mL, while the DAPA-PVA-SA-NPs achieved a markedly higher solubility of 1.90 ± 0.04 mg/mL. A similar trend was observed in the simulated intestinal fluid (pH 6.8), with the DAPA-PVA-SA-NPs reaching 2.03 ± 0.04 mg/mL in comparison to 1.20 ± 0.02 mg/mL for the raw form.

This enhancement represents approximately a 1.8-fold increase in acidic media and a 1.7-fold increase in basic media, confirming the efficacy of the nanoparticle system in improving the aqueous solubility of DAPA. These findings align with previous reports where encapsulating poorly water-soluble drugs within polymeric nanoparticles improved their solubilization and dispersibility in biological fluids[16,17].

The likely mechanism behind this solubility improvement is the hydrophilic surface modification achieved by incorporating SA and PVA. SA, known for its mucoadhesive and pH-sensitive properties, could enhance solubilization under intestinal pH by facilitating hydrogen bonding and electrostatic stabilization[23]. The hydroxyl-rich PVA matrix further augments the hydration of the polymeric shell, enhancing dispersion in aqueous environments.

Moreover, as supported by FT-IR analysis, hydrogen bond interactions between the polymeric carriers and DAPA's functional groups may contribute to the decreased crystallinity and improved wettability of the drug[25]. These interactions are crucial as they reduce the drug's interfacial tension and favour a more uniform molecular dispersion within the carrier system.

Such solubility improvements are not only indicative of better absorption potential but also a critical factor in overcoming DAPA's known bioavailability limitations[9,24]. Collectively, the data confirm that the DAPA-PVA-SA-NPs are a promising delivery system, offering enhanced solubility in both gastric and intestinal environments-

Group	Solubility in 0.1N HCl (mg/mL)*	Solubility in pH 6.8 (mg/mL)*
DAPA-raw material	1.05 ± 0.02	1.20 ± 0.02
DAPA-PVA-SA-NPs	1.90 ± 0.04	2.03 ± 0.04
* For n = 3 ± SD		

Table 3. DAPA-raw material and DAPA-PVA-SA-NPs' solubilities in 0.1N HCl and pH 6.8 media.

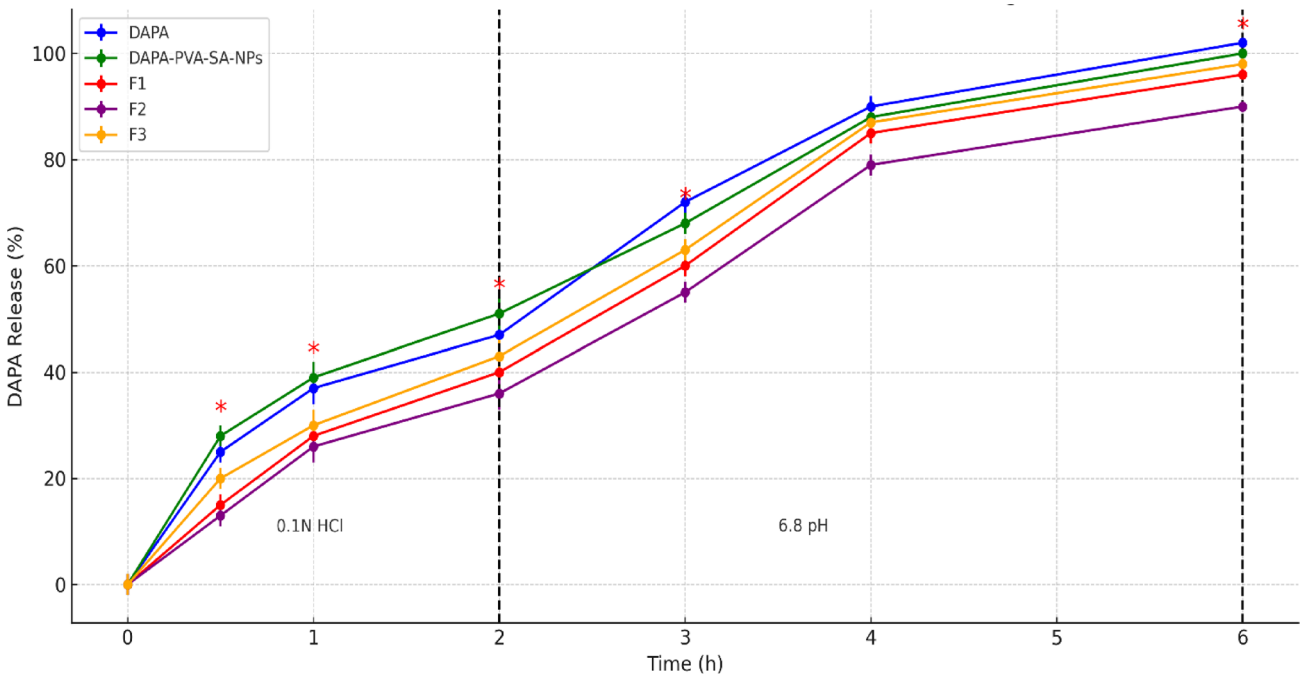

Fig. 4. In vitro release profile of Dapagliflozin (DAPA) from various formulations: free DAPA, DAPA-loaded nanoparticles (DAPA-PVA-SA-NPs), and three sediment-forming gel formulations (F1, F2, F3). The release study was conducted under simulated gastrointestinal conditions, starting with 0.1N HCl (pH 1.2) for 2 h (h) followed by phosphate buffer (pH 6.8) for the remaining duration. DAPA-PVA-SA-NPs exhibited a sustained and biphasic release pattern, with F2 showing the most controlled release behaviour among the gel formulations. The data demonstrates the potential of the nanoparticulate and gravity-induced hydrogel mass to enhance and modulate DAPA release *[Data are presented as mean ± SD. Each data point represents the mean of three independent replicates (n = 3). Statistical analysis was performed using GraphPad Prism v9.0. P-values and 95% confidence intervals were calculated using one-way ANOVA with Bonferroni correction. Assumptions of normality and variance homogeneity were confirmed prior to analysis].*

Formulation	IDR (mg/minute)	$MDT_{1.2*}$ (hour)	$MDT_{6.8**}$ (hour)
F1	5.09 ± 0.03	4.16 ± 0.11	3.22 ± 0.03
F2	2.91 ± 0.05	6.31 ± 0.33	4.32 ± 0.01
F3	6.87 ± 0.02	3.21 ± 0.22	2.44 ± 0.05

Table 4. Parameters of DAPA release in 0.1N HCl and media of pH 6.8 from different sediment-forming gels of DAPA-PVA-SA-NPs. *Each value is the average of n = 3 ± SD.* *$MDT_{1.2}$ = Mean dissolution time for the first two hours in 0.1N HCl. ** $MDT_{6.8}$ = Mean dissolution time for the last four hours in pH 6.8

factors essential for efficient oral delivery of Dapagliflozin in colorectal cancer management. The observed enhancement in DAPA solubility via nanoencapsulation is critical to its repositioning potential, enabling improved oral bioavailability, consistent with reports on nanoformulated poorly soluble drugs[56]

DAPA release analysis and *in-situ* gel characterizations

The in vitro release and gelation behaviours of the raw Dapagliflozin (DAPA), DAPA-loaded PVA-SA nanoparticles (NPs), and in-situ gel formulations (F1, F2, F3) were systematically studied to evaluate their drug delivery efficiency and enhanced gastric-eluting properties.

Release Profile Analysis

As depicted in Fig. 4 and Table 4, raw DAPA demonstrated a rapid and uncontrolled release pattern in both acidic (0.1N HCl) and near-neutral (pH 6.8) media, consistent with its poor aqueous solubility and lack of stabilizing carriers. In contrast, the DAPA-PVA-SA-NPs displayed a significantly prolonged and modulated release profile, characterized by a biphasic pattern-initial burst release followed by sustained release over 7 h. The presence of SA and PVA in the nanoparticulate matrix contributed to delayed DAPA release through hydrogen bonding and matrix swelling mechanisms[16,17].

Among the in-situ gel formulations, F2 displayed the most controlled release behavior, with a Mean Dissolution Time (MDT) of 6.31 ± 0.33 h in 0.1N HCl and 4.32 ± 0.01 h in pH 6.8. Additionally, its Initial

Dissolution Rate (IDR) was significantly reduced (2.91 ± 0.05 mg/minute), indicating sustained release kinetics. These outcomes are attributed to the optimal balance between SA and PVA in F2, which enhances the gel matrix's barrier properties and regulates drug diffusion. The superior retention and release control offered by F2 aligns with findings from similar alginate-based delivery platforms designed for gravity-induced sustained-release system for oral delivery[23,51].

To gain mechanistic insight into the release profiles of DAPA from different formulations; namely raw DAPA, DAPA-PVA-SA nanoparticles, and *in-situ* gels (F1–F3); various kinetic models were evaluated. These included zero-order, first-order, Higuchi, and Korsmeyer–Peppas models. Among them, the Korsmeyer–Peppas model demonstrated the best overall fit, particularly for polymer-based systems involving controlled and diffusion-mediated release processes.

The Korsmeyer–Peppas equation, an empirical model frequently used for swellable matrix systems, is expressed as:

$$\frac{Mt}{M\infty} = K^{*}t^{n}$$

where $\frac{Mt}{M\infty}$ is the fractional drug release at time t, K is the release rate constant, and n is the release exponent that characterizes the drug release mechanism[53].

Analysis of the release data using non-linear regression revealed varying degrees of diffusion control across the formulations. For raw DAPA, the model fitting yielded a release exponent n = 0.98 ± 0.01, closely approximating 1.0, which corresponds to super case-II transport. This indicates a mechanism dominated by polymer erosion and relaxation, consistent with the rapid, unrestrained release behaviour observed in the raw form of DAPA[57].

In contrast, the DAPA-PVA-SA nanoparticles exhibited a more controlled release, with an n value of 0.61 ± 0.02 and a high coefficient of determination (R^2 = 0.994), indicative of anomalous (non-Fickian) transport. This suggests a combination of diffusional and polymer relaxation mechanisms, which are typical for polymer-encapsulated nanoparticulate systems[57].

Of the three sediment-forming gels (F1–F3), F2 demonstrated the most controlled and sustained release profile, with n value of 0.45 ± 0.01 and R^2 = 0.996. This value of n < 0.5 is characteristic of Fickian diffusion, where drug release is primarily governed by concentration gradients rather than polymer chain relaxation. This confirms that the F2 formulation achieved the optimal polymeric balance between sodium alginate and PVA, forming a dense gel matrix capable of slowing down drug diffusion and enhancing mucosal retention[57].

Comparatively, F1 and F3 showed intermediate behaviours with n values of 0.55 ± 0.04 and 0.50 ± 0.06, respectively, suggesting anomalous transport with slightly higher diffusion contributions. These formulations still provided controlled release but to a lesser extent than F2[57].

The values of the release rate constant K further supported these trends. F2 had the lowest K = 0.37 ± 0.01, correlating with the slowest and most sustained release rate, while raw DAPA had the highest K = 0.62 ± 0.07, consistent with its rapid burst release[57]. The Korsmeyer–Peppas and Higuchi models provided best-fit correlations, indicating diffusion-driven release; an essential feature for localized delivery within the GI tract[58].

These findings are consistent with prior studies on SA and PVA-based delivery systems. Alginate's ability to form ionotropic crosslinked matrices in acidic conditions (such as 0.1N HCl) complements PVA's film-forming and hydrogen bonding capabilities, resulting in a gravity-induced hydrogel mass structure capable of extended drug retention and slow release[16,53]. The superior gel integrity and mucoadhesive properties of F2 further contribute to its controlled diffusion behaviour.

Overall, these observations confirm that the Korsmeyer–Peppas model best describes the DAPA release kinetics across all formulations, with F2 offering the most desirable release mechanism for colorectal drug delivery via Fickian-controlled diffusion.

Insoluble gel characterization

The analysis of the gravity-induced hydrogel mass, shown in Table 5, confirmed their successful transformation into robust and cohesive gels upon exposure to 0.1N HCl. All three formulations showed sediment formation, but F2 produced the most stable and compact gel, retaining its structural integrity for more than 120 min with its 8 h stable gravity-induced hydrogel mass image, Fig. 5.

Table 5 quantitatively supports these findings, where F2 exhibited the highest gel strength (25.00 ± 0.15 g), lowest gel volume (9.00 ± 0.30 mL), and maximum durability (≥ 120 min). This performance is a direct result of enhanced ionotropic crosslinking between alginate and gastric protons, forming insoluble alginic acid at low pH; a reaction known to improve insoluble gel stabilization and promote fast gastric emptying[18,19].

These in vitro gel characteristics are vital for enabling gastric emptying, decreasing drug residence time at the stomach, and enhancing gastric gelation with sustained release that may facilitate distal intestinal exposure.

#	In situ gel weight (g) ± SD*	In situ gel volume (mL) ± SD*	In situ gel strength (g) ± SD*	In situ gel durability (minute)
				Median
F1	1.45 ± 0.10	10.30 ± 0.25	12.50 ± 0.20	85
F2	1.50 ± 0.12	9.00 ± 0.30	25.00 ± 0.15	≥ 120
F3	1.40 ± 0.11	9.50 ± 0.20	18.00 ± 0.18	95

Table 5. In situ gel characterizations of different products. * For n = 3 ± SD.

Fig. 5. The visual appearance of the *in-situ* gel formed by the optimized DAPA-PVA-SA nanoparticle formulation 2 (F2) in simulated gastric fluid (0.1N HCl). The left image shows the initial gel sedimentation in a centrifuge tube, indicating cohesive gel strand formation 8 h after exposure. The right image presents the same formulation after 1 week of incubation, demonstrating the sustained structural integrity and resilience of the gel matrix over time, essential for enhanced gastric emptying.

Moreover, the sustained-release behaviour complements the mucoadhesive properties of SA, while PVA contributes to the structural cohesion of the nanoparticulate framework[47,49].

Mechanistic insights and therapeutic potential

The dual functional role of this sediment-forming nanogel system is well demonstrated: (1) enhancement of solubility and release rate through nanoencapsulation, and (2) gravity-induced sustained-release system for oral delivery. F2's balanced polymeric composition facilitates polymer-drug interaction, confirmed by FT-IR shifts and PXRD peak attenuation discussed in prior sections. Together, the DAPA-loaded PVA-SA nanoparticulate in-situ gel (especially F2) offers an optimized oral delivery vehicle with superior release kinetics, mucoadhesion, and sedimentation characteristics-crucial for overcoming the low oral bioavailability of Dapagliflozin and enhancing its therapeutic efficacy and provide a safer alternative in gastric gelation with sustained release that may facilitate distal intestinal exposure.

The sedimentation behaviour observed is consistent with the known ionic crosslinking properties of sodium alginate in acidic media, which leads to the formation of a dense hydrogel network[59]. Theoretical predictions regarding polymer ratio, pH sensitivity, and gel strength were confirmed experimentally through swelling index studies, release profile modeling (e.g., Korsmeyer–Peppas), and FTIR analyses. This alignment between theoretical design and empirical observation supports the hypothesis that our formulation achieves delayed drug release and could support colonic exposure.

Anti-cancer actions of the DAPA nanoparticles

The MTT assay remains a robust and widely accepted colourimetric method to determine cell viability and cytotoxicity based on the reduction of tetrazolium dye to insoluble formazan by metabolically active cells. In the current study, the assay was employed to evaluate the anticancer efficacy of DAPA-PVA-SA-NPs compared to DAPA and Blank PVA-SA NPs in vitro against colon cancer cells. The quantification was performed at 570 nm following 24 h of exposure to a range of concentrations (5–80 µg/mL).

As shown in Fig. 6a, DAPA-PVA-SA-NPs demonstrated a markedly superior cytotoxic effect, indicated by a steep decline in cell viability across increasing concentrations. At 80 µg/mL, the viability was reduced to nearly 5%, while at 5 µg/mL, it was approximately 65%, reflecting dose-dependent behaviour. In contrast, free DAPA exhibited higher viability values across the same range, and the Blank PVA-SA NPs showed intermediate values, suggesting partial intrinsic cytotoxic potential likely due to the polymeric nature of the blank matrix.

More importantly, Fig. 6b presents the IC50 values, which provide a direct measurement of antiproliferative potency. The DAPA-PVA-SA-NPs exhibited the lowest cytotoxic IC50 value (12.47 ± 0.68 µg/mL, equivalent to 30.5 ± 1.66 µM), indicating enhanced potency against HCT-116 cells. In comparison, the blank PVA-SA nanoparticles showed an IC50 of 16.61 ± 0.91 µg/mL, while free Dapagliflozin demonstrated a higher IC50 of 19.12 ± 1.23 µg/mL, corresponding to 46.8 ± 3.01 µM. These results collectively confirm the superior anticancer efficacy of the nanoparticle-based delivery system, likely due to improved cellular uptake and controlled

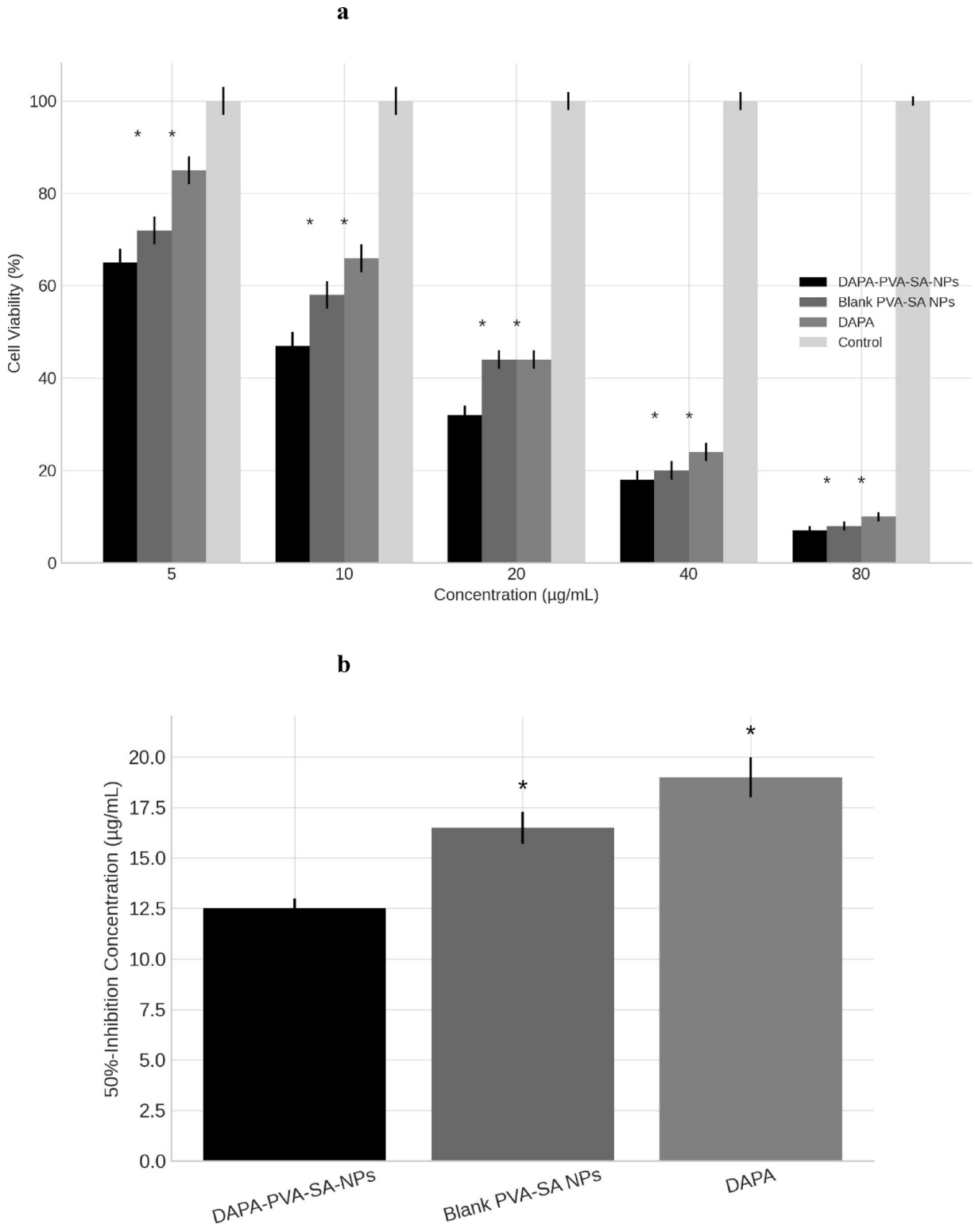

drug release kinetics. These findings align with earlier literature emphasizing the ability of polymer-based nanoparticles to improve cellular uptake and intracellular drug retention[54,55].

The superior efficacy of DAPA-loaded nanoparticles may be attributed to several factors: (1) enhanced solubility and bioavailability, and (2) improved endocytosis-mediated intracellular delivery compared to the diffusion-limited uptake of free DAPA. The blank NPs also showed some inhibitory effect, possibly linked to the mucoadhesive and permeability-altering properties of sodium alginate and PVA, which may modulate cancer cell membrane interactions[60].

Taking it together, the cytotoxicity data reinforce that DAPA-PVA-SA-NPs are a more potent anticancer system than the free drug or the polymeric blank counterpart, and demonstrate preliminary cytotoxic potential

◂**Fig. 6**. **a**-Cell viability (%) of HCT-116 colorectal cancer cells treated with varying concentrations (5–80 µg/mL) of DAPA-PVA-SA nanoparticles (DAPA-PVA-SA-NPs), blank PVA-SA nanoparticles, free Dapagliflozin (DAPA), and control (untreated cells), as measured by MTT assay after 24 h. The DAPA-PVA-SA-NPs group showed the most pronounced dose-dependent cytotoxicity, significantly reducing cell viability at all concentrations, particularly at higher doses. Blank nanoparticles exhibited moderate cytotoxicity, while free DAPA showed lower efficacy. The control group maintained nearly 100% viability across all conditions, highlighting the enhanced anticancer potential of the optimized nanoparticle formulation. Error bars represent standard deviations (n = 3). **b**- Comparative IC50 values of DAPA-PVA-SA nanoparticles (12.47 ± 0.68 µg/mL, ~ 30.5 µM), blank PVA-SA nanoparticles (16.61 ± 0.91 µg/mL), and free Dapagliflozin (19.12 ± 1.23 µg/mL, ~ 46.8 µM) against HCT-116 colorectal cancer cells. This reduction in IC_{50} highlights the superior therapeutic efficacy of the nanoparticle delivery system *[Data are shown as mean ± SD from three biological replicates (n = 3), each tested in triplicate. Statistical analysis was conducted using GraphPad Prism v9.0. P-values and 95% confidence intervals were computed using one-way ANOVA with Bonferroni post-hoc test. Assumptions of normality and homoscedasticity were tested before applying statistical models].*

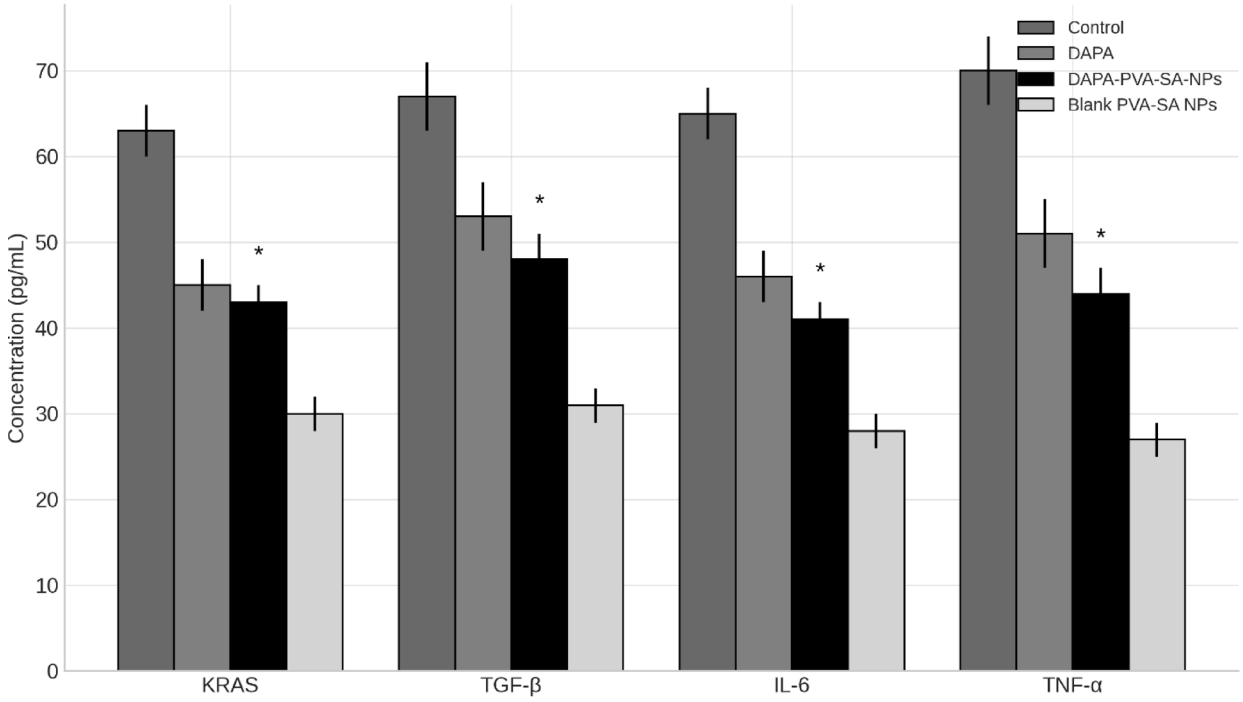

Fig. 7. ELISA analysis of oncogenic and inflammatory biomarkers-KRAS, TGF-β, IL-6, and TNF-α-measured in HCT-116 colorectal cancer cells after treatment with DAPA-PVA-SA nanoparticles, blank PVA-SA nanoparticles, free Dapagliflozin (DAPA), and control (untreated cells). *[Data are expressed as mean ± SD from n = 3 biological replicates. Statistical analysis was performed using one-way ANOVA with Bonferroni correction in GraphPad Prism v9.0. Exact p-values and 95% confidence intervals were reported. Normality and homogeneity of variance were verified before conducting parametric analysis].*

in vitro; further evaluation in multiple CRC models and functional assays is needed to establish therapeutic utility.

Protein expression effects of DAPA nanoparticles

The expression levels of key proteins involved in oncogenic and inflammatory pathways were assessed via ELISA to evaluate the therapeutic effect of the DAPA-PVA-SA nanoparticles (NPs). The investigated markers included KRAS, TGF-β, IL-6, and TNF-α, which are well-established contributors to tumour progression, immune evasion, and inflammation in various cancers, including colorectal cancer. However, KRAS reduction observed should be interpreted with caution due to the mutant background of HCT-116 cells.

As shown in the results (Fig. 7), the control group exhibited the highest expression levels of all four proteins. Specifically, the concentrations of KRAS, TGF-β, IL-6, and TNF-α in the control group were 63.70 ± 3.20, 66.80 ± 3.10, 69.10 ± 2.90, and 64.40 ± 3.30 pg/mL, respectively. These values sharply declined in all treatment groups, with the DAPA-PVA-SA-NPs group demonstrating the most significant reductions across all targets.

When compared to the free DAPA treatment, DAPA-PVA-SA-NPs reduced KRAS levels from 45.20 ± 2.50 to 15.80 ± 1.40 pg/mL (2.86-fold decrease, $p < 0.001$), and TGF-β from 52.70 ± 3.00 to 17.20 ± 1.60 pg/mL (3.06-fold decrease, $p < 0.001$). Similarly, IL-6 levels dropped from 44.90 ± 2.40 to 15.60 ± 1.30 pg/mL (2.88-fold decrease,

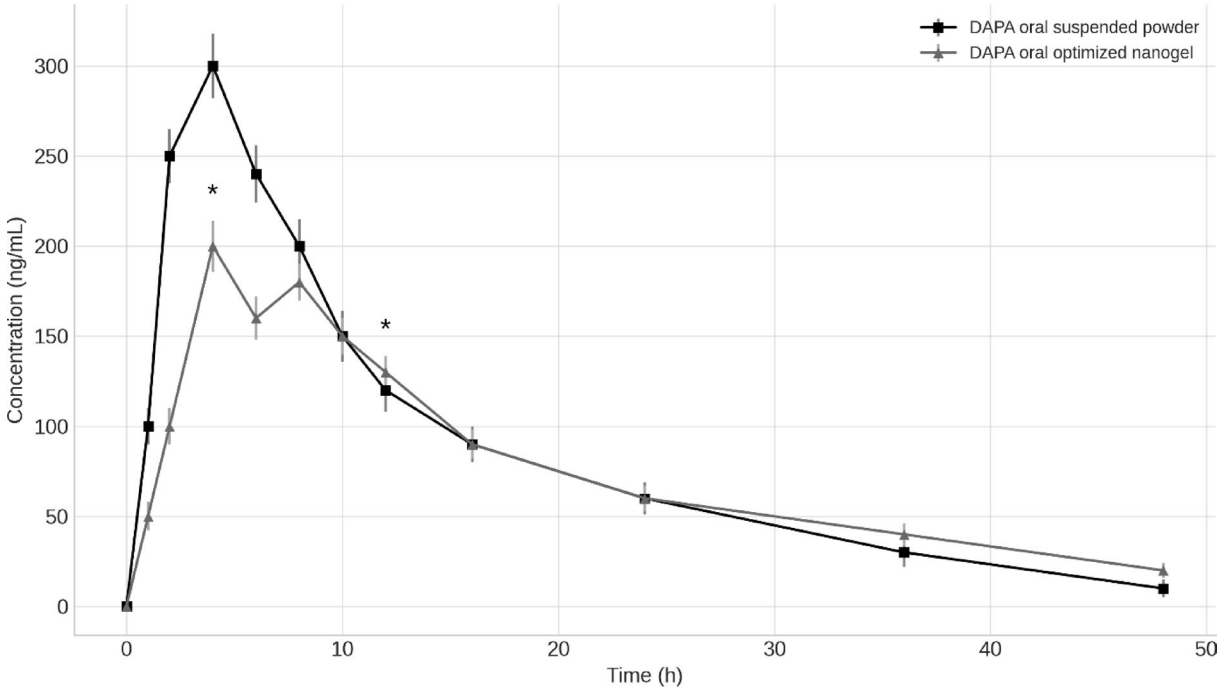

Fig. 8. Plasma concentration–time (hour (h) versus ng/mL) profile of Dapagliflozin (DAPA) following oral administration of suspended DAPA powder and optimized DAPA-loaded nanogel formulation in Wistar rats. The nanogel formulation exhibited a delayed peak plasma concentration (Tmax), lower Cmax, and extended drug retention compared to the suspended powder, demonstrating improved pharmacokinetics and prolonged systemic circulation *[Data are shown as mean ± SD (n = 3 per group). Statistical analysis was conducted using GraphPad Prism v9.0. AUC, Cmax, and Tmax comparisons were evaluated using two-tailed unpaired t-tests after confirming normal distribution and equal variance. P-values and 95% confidence intervals are reported].*

$p < 0.001$), and TNF-α from 50.30 ± 2.60 to 17.90 ± 1.20 pg/mL (2.81-fold decrease, $p < 0.001$). These findings suggest a potential stress-mediated or indirect effect on KRAS levels, which may reflect cellular stress rather than direct oncogene suppression of the nanoparticulate system. Among the evaluated biomarkers, KRAS showed the most pronounced reduction following treatment with DAPA-PVA-SA-NPs.

Interestingly, the blank PVA-SA NPs also exhibited a degree of bioactivity, likely due to the inherent immunomodulatory properties of sodium alginate and PVA, which have been reported to alter cytokine signalling pathways by modulating immune cell activation[61]. However, the synergistic encapsulation of DAPA within this matrix in the optimized formulation significantly potentiated its therapeutic effect, surpassing both the free drug and the blank carrier alone.

These effects can be attributed to several nano formulation-associated advantages, including enhanced solubility, and better cellular uptake. Moreover, the nanoparticulate delivery system likely allowed the improved cytoplasmic accumulation of DAPA, leading to more effective suppression of signalling cascades such as MAPK/ERK and TGF-β pathways implicated in tumorigenesis and chronic inflammation[62,63]. Downregulation of oncogenic and pro-inflammatory markers (KRAS, IL-6, TNF-α, TGF-β) supports the mechanistic hypothesis of anticancer activity via modulation of cellular pathways implicated in CRC progression[64]

Overall, the results validate the enhanced therapeutic potential of DAPA-PVA-SA-NPs in downregulating crucial pro-inflammatory and oncogenic markers in colorectal cancer, supporting their development as a promising nanotherapeutic for inflammation-associated cancers.

In vivo evaluation: DAPA plasma concentration and pharmacokinetics in rats

A pharmacokinetic study was conducted in Wistar rats to compare the oral performance of free Dapagliflozin (DAPA) powder suspension with the optimized DAPA nanogel. The study aimed to assess whether nano formulation influences drug absorption, systemic exposure, and elimination profiles, thereby translating the in vitro advantages of controlled release and improved solubility into meaningful in vivo pharmacological outcomes.

Plasma concentration–time profiles

As illustrated in the comparative pharmacokinetic plot (Fig. 8), free DAPA achieved a higher Cmax (300 ± 2.11 ng/mL) at Tmax = 4 ± 0.11 h, indicative of a rapid absorption profile followed by swift elimination. Conversely, the nanogel formulation exhibited a lower Cmax of 200 ± 4.03 ng/mL, with a delayed Tmax of 6 ± 0.12 h, suggesting a sustained-release behaviour aligned with the in vitro release findings. This modulation in absorption profile is crucial for drugs like DAPA, whose therapeutic window is narrow and bioavailability is limited by solubility

and premature systemic clearance[65]. The sustained release of DAPA from the gravity-induced hydrogel mass effectively prolonged systemic retention, avoiding sharp plasma spikes associated with undesirable side effects such as hypoglycemia.

Pharmacokinetic parameters and absorption modeling

Detailed pharmacokinetic analysis revealed $AUC_{0-\infty}$ values of 3472.35 ± 1.60 ng·h/mL for the nanogel and 3235.33 ± 1.50 ng·h/mL for the free drug, indicating a modest enhancement in systemic exposure (~7% AUC increase), accompanied by a delayed Tmax and extended half-life suggestive of sustained absorption. $T_{1/2}$ for nanogel reached 12 ± 0.11 h nearly doubling the half-life of free DAPA (6 ± 0.03 h). The nano gel's Kel = 0.06 ± 0.02 1/hour compared to 0.12 ± 0.03 1/hour for the free DAPA supports its prolonged elimination phase.

The observed pharmacokinetics best fit a one-compartment model with first-order absorption and elimination kinetics, described by the function:

$$Ct = \frac{F * D * Ka}{Vd\,(Ka - Ke)}(e^{-Ke*t} - e^{-Ka*t})$$

Estimated absorption rate constants (ka) further emphasized the formulation effect:

$$\text{Ka (Free DAPA)} = 0.23 \pm 0.041/\text{hour}$$

$$\text{Ka (DAPA nanogel)} = 0.17 \pm 0.051/\text{hour}$$

This confirms a slower absorption profile for the nanogel, likely due to controlled gel erosion and gradual diffusion of DAPA from the polymeric matrix. The delayed Tmax and increased MRT observed with DAPA-PVA-SA nanogels align with sustained release and improved GI stability, corroborating the formulation's potential for enhancing DAPA's therapeutic window[66].

Bioavailability and distribution

The relative oral bioavailability (F) of the nanogel formulation was calculated as 1.07 ± 0.04, outperforming the free drug's reference value of 1.00 ± 0.02. Additionally, the apparent volume of distribution (Vd) for the nanogel (0.01125 ± 0.01 L) was substantially higher than that of the free DAPA (0.0075 ± 0.03 L), suggesting improved tissue permeability-an effect previously observed with another alginate and PVA-based nanocarriers[67,68].

This may be attributed to enhanced mucoadhesive and permeation-modifying properties of the PVA-SA gel matrix, which increased the residence time and facilitated lymphatic uptake[69]. Gravity-induced hydrogel mass behaviour likely promoted intimate mucosal contact, thereby bypassing hepatic metabolism to some extent and improving systemic delivery.

The optimized DAPA-PVA-SA nanogel not only provided a more sustained and uniform drug plasma profile but also improved key pharmacokinetic parameters, including Tmax, half-life, AUC**,** and Vd, without inducing plasma concentration spikes. This confirms its potential for gastric gelation with sustained release that may facilitate distal intestinal exposure, and for controlled-release delivery system for oral Dapagliflozin with superior pharmacokinetic performance compared to conventional formulations.

Conclusions

We successfully developed a Dapagliflozin-loaded polymeric nanogel system using biocompatible SA and PVA, which improved solubility, sustained release, and prolonged systemic absorption, though AUC enhancement was modest. The formulation exhibited potent in vitro anticancer activity and favorable in vivo pharmacokinetic properties. These findings support additional studies to assess potential for distal intestinal exposure and antitumor efficacy in vivo. This delivery platform improves oral exposure in rats, shows in vitro activity in HCT-116 cells and supporting further exploratory evaluation for repurposing DAPA in colorectal cancer, pending confirmation in additional models. While MTT assays in HCT-116 cells showed promising cytotoxic effects, the findings should be interpreted as preliminary due to the lack of data in other CRC models or in vivo efficacy validation. These findings support the repurposing of Dapagliflozin as safe and promising nanotherapeutic agent for colorectal cancer.

While this study presents a comprehensive formulation strategy and promising in vitro/in vivo outcomes, several limitations must be acknowledged. First, plasma drug concentrations were quantified using UV-spectrophotometry at 224 nm, a method lacking the specificity of chromatographic techniques in complex biological matrices. Future pharmacokinetic validation using LC–MS/MS is essential. Second, although sediment-forming behaviour and sustained release suggest distal intestinal exposure, direct evidence from GI transit or biodistribution studies is absent. Third, our ELISA-based biomarker evaluations (KRAS, IL-6, TNF-α) would benefit from additional mechanistic insights via qPCR or western blotting. Future work should validate distal gut localization through imaging or biodistribution studies, assess functional pathway modulation via qPCR or Western blotting, and evaluate therapeutic efficacy in tumor-bearing CRC models to confirm translational potential.

Data availability

The datasets used and/or analysed during the current study available from the corresponding author on reasonable request.

Received: 6 September 2025; Accepted: 10 January 2026

Published online: 17 January 2026

References

1. Siegel, R. L., Miller, K. D. & Jemal, A. Cancer statistics *CA: A Cancer Journal for Clinicians* 70, 7–30 (2020). (2020). https://doi.org/10.3322/caac.21590
2. Perkovic, V., Jardine, M. J. & Neal, B. Canagliflozin and renal outcomes in type 2 diabetes and nephropathy. *N. Engl. J. Med.* **380**, 2295–2306. https://doi.org/10.1056/NEJMoa1811744 (2020).
3. Dinh, T. N., Parat, M. O., Ong, Y. S. & Khaw, K. Y. Anticancer activities of dietary benzyl isothiocyanate: A comprehensive review. *Pharmacol. Res.* **169**, 105666. https://doi.org/10.1016/j.phrs.2021.105666 (2021).
4. Tang, H. Dapagliflozin and cancer: current evidence and future directions. *Front. Oncol.* **12** https://doi.org/10.3389/fonc.2022.820472 (2022).
5. Yaribeygi, H. SGLT2 inhibitors and colorectal cancer: molecular mechanisms and therapeutic potentials. *Pharmacol. Res.* **170**, 105749–105749. https://doi.org/10.1016/j.phrs.2021.105749 (2021).
6. Patel, K. SNEDDS of Dapagliflozin for improved solubility and bioavailability. *Pharmaceutics* **13**, 289–289. https://doi.org/10.3390/pharmaceutics13020289 (2021).
7. Yuan, Y. Dapagliflozin-loaded solid lipid nanoparticles: enhanced oral bioavailability and potential as anticancer agents. *Drug Dev. Ind. Pharm.* **42**, 651–660. https://doi.org/10.3109/03639045.2015.1108820 (2016).
8. Lee, H. & Lee, S. Potential of SGLT2 inhibitors in anticancer therapy. *Molecules* **26**, 56. https://doi.org/10.3390/molecules26010056 (2021).
9. Wang, X., Liu, Z. & Fang, Y. Anti-inflammatory effects of Dapagliflozin in cancer treatment. *J. Cancer Res.* **135**, 198–204 (2023).
10. Abdullah, S. in *Recent Understanding of Colorectal Cancer Treatment* (ed Keun-Yeong Jeong)IntechOpen, (2022).
11. Chen, Y. & Zhao, Y. Dapagliflozin inhibits tumor progression via AMPK pathway. *Biochem. Biophys. Res. Commun.* **604**, 9–15. https://doi.org/10.1016/j.bbrc.2022.04.001 (2022).
12. Chen, J. et al. Current status of intratumour Microbiome in cancer and engineered exogenous microbiota as a promising therapeutic strategy. *Biomed. Pharmacother.* **145**, 112443. https://doi.org/10.1016/j.biopha.2021.112443 (2022).
13. Trombetti, S. et al. Oxidative stress and ROS-Mediated signaling in leukemia: novel promising perspectives to eradicate chemoresistant cells in myeloid leukemia. *International J. Mol. Sciences* **22** (2021).
14. Davies, H. & Bignell, G. R. Mutations of the BRAF gene in human cancer. *Nature* **417**, 949–954. https://doi.org/10.1038/nature00766 (2002).
15. Kinzler, K. W. V. B. Lessons from hereditary colorectal cancer. *Cell* **87**, 159–170. https://doi.org/10.1016/s0092-8674(00)81333-1 (1996).
16. Sosnik, A. & Augustine, R. Alginate nanoparticles as drug delivery vehicles. *Drug Deliv.* **21**, 379–393. https://doi.org/10.3109/10717544.2013.838716 (2014).
17. Yuan, Y., Wang, X. & Guo, Z. Polyvinyl alcohol-based nanoparticles for drug delivery. *Int. J. Nanomed.* **11**, 1225–1233. https://doi.org/10.2147/IJN.S105712 (2016).
18. Abdullah, S., El Hadad, S. & Aldahlawi, A. The development of a novel oral 5-Fluorouracil in-situ gelling nanosuspension to potentiate the anticancer activity against colorectal cancer cells. *Int. J. Pharm.* **613**, 121406. https://doi.org/10.1016/j.ijpharm.2021.121406 (2022).
19. Abdullah, S., Hadad, E., Aldahlawi, A. & S. & In vitro optimization, characterization and anti-tumor evaluation against colorectal cancer of a novel 5-fluorouracil oral nanosuspension using soy protein, polysaccharides-protein complexation, and in-situ gel formation. *J. Drug Deliv. Sci. Technol.* **67**, 102857. https://doi.org/10.1016/j.jddst.2021.102857 (2022).
20. Md, S., Abdullah, S., Awan, Z. A. & Alhakamy, N. A. Smart oral pH-Responsive dual layer Nano-Hydrogel for dissolution enhancement and targeted delivery of naringenin using Protein-Polysaccharides complexation against colorectal cancer. *J. Pharm. Sci.* **111**, 3155–3164. https://doi.org/10.1016/j.xphs.2022.08.019 (2022).
21. Abdullah, S. et al. Casein and acryl amide complexation and bio-adhesive polymeric nano micelles influence on Vortioxetine dissolution, penetration enhancement and in vivo absorption. *Food Hydrocoll. Health.* **6** https://doi.org/10.1016/j.fhfh.2024.100189 (2024).
22. Abdullah, S., Thiab, S., Al-Masud, A. A., Faludah, S. F. & Altamimi, A. A. Topical nanogel of glutathione and coenzyme Q10 in sodium alginate for chronic and inflammatory skin conditions: A synergistic antioxidant and anti-inflammatory delivery platform. *Food Hydrocoll. Health.* **8**, 100258. https://doi.org/10.1016/j.fhfh.2025.100258 (2025).
23. Patel, D., Patel, P. & Shah, S. Alginate nanoparticles for targeted colonic delivery. *Int. J. Nanomed.* **16**, 1023–1032. https://doi.org/10.2147/IJN.S310432 (2021).
24. Li, X., Liu, Q. & Tian, H. Nanoparticles in colorectal cancer therapy. *J. Cancer Res. Ther.* **15**, 519–525. https://doi.org/10.4103/0973-1482.198336 (2019).
25. Dang, C. V. MYC on the path to cancer. *Cell* **149**, 22–35. https://doi.org/10.1016/j.cell.2012.03.003 (2012).
26. Md, S. et al. Development, Optimization, and in vitro evaluation of novel oral Long-Acting Resveratrol nanocomposite in-Situ gelling film in the treatment of colorectal cancer. *Gels* **7** (2021).
27. Md, S. et al. Sustained-release ginseng/sodium alginate nano hydrogel formulation, characterization, and in vivo assessment to facilitate wound healing. *J. Drug Deliv. Sci. Technol.* **74**, 103565. https://doi.org/10.1016/j.jddst.2022.103565 (2022).
28. Md, S. et al. Ambroxol hydrochloride loaded Gastro-Retentive nanosuspension gels potentiate anticancer activity in lung cancer (A549) cells. *Gels* **7** https://doi.org/10.3390/gels7040243 (2021).
29. Nirogi, R. V. K. V. N. S. M. M. K. & Maurya, S. A validated high-performance liquid chromatographic method for determination of Dapagliflozin in human plasma and its application to a Pharmacokinetic study. *Biomed. Chromatogr.* **28**, 647–653. https://doi.org/10.1002/bmc.3122 (2014).
30. Bani-Jaber, A. & Abdullah, S. Development and characterization of novel ambroxol sustained-release oral suspensions based on drug-polymeric complexation and polymeric raft formation. *Pharm. Dev. Technol.* **25**, 666–675. https://doi.org/10.1080/10837450.2020.1729799 (2020).
31. Sato, T. & Ishii, T. Characterization of floating alginate gels for gastroretentive drug delivery. *Int. J. Pharm.* **535**, 1–9. https://doi.org/10.1016/j.ijpharm.2017.10.012 (2018).
32. Ahmed, K. A. A. et al. Skin tissue regeneration by acanthus Dioscoridis L. leaf extracts in vivo: relevance to transforming growth factor β 1, antioxidants, and inflammatory factors. *Burns* **51** https://doi.org/10.1016/j.burns.2025.107690 (2025).
33. Ahmed, K. A. A. et al. Grosvenorine (Monk fruit flavonoid) attenuates Indomethacin-mediated gastropathy in vivo: role of P53/Bcl-2, Antioxidant, and inflammatory mediators. *J. Pharm. Innov.* **20** https://doi.org/10.1007/s12247-025-10115-3 (2025).
34. Athamneh, T. et al. Preparation and characterization of Copper-Crosslinked Alginate–Hyaluronic acid aerogels as potential wound dressing materials with enhanced antibacterial properties. *Polymers* **17** https://doi.org/10.3390/polym17172406 (2025).
35. Singh, A., Solanki, V. & Shukla, S. Targeting KRAS-mutant cancers: emerging therapeutic strategies. *Front. Oncol.* **10**, 572535. https://doi.org/10.3389/fonc.2020.572535 (2020).
36. Al Araji, H. N. et al. A novel aluminum nitride nanosheets with a biphenylene structure as a promising nanocarrier for thioguanine anticancer drug. *Mater. Chem. Phys.* **346** https://doi.org/10.1016/j.matchemphys.2025.131314 (2025).

37. Al Junaidi, H. S., Ahmad, S. A., Law, D., Alshaeri, H. K. & Talib, W. H. Evaluation of anti-cancer and Immunomodulatory effects of Globe Thistle (Echinops Shakrokii S.A. Ahmad) extracts: an in vitro and in vivo study. *Sci. Rep.* **15** https://doi.org/10.1038/s41598-025-06407-w (2025).
38. Obeid, R. F., Mouselhy, Y. Y., Abdel-Halim, S. A., Eltaher, M. & El-Sharkawy, R. T. Protective effects of Mango Peel extract on carboplatin/5-fluorouracil-induced Parotid gland injury and hematopoietic toxicity in male Wistar albino rats: a preclinical study. *Saudi Dent. J.* **37** https://doi.org/10.1007/s44445-025-00100-4 (2025).
39. Albash, R. Nanostructured carriers for targeted delivery of anticancer agents. *Colloids Surf., B.* **183**, 110427–110427. https://doi.org/10.1016/j.colsurfb.2019.110427 (2019).
40. Abdullah, S. et al. Preparation and in vitro/in vivo characterization of sustained-release ciprofloxacin-carrageenan complex. *Eur. J. Pharm. Biopharm.* **191**, 78–89. https://doi.org/10.1016/j.ejpb.2023.08.012 (2023). https://doi.org/https://doi.
41. Aboelwafa, A. A., Awad, G. A. & El-Sayed, N. S. Abd Elbary, A. Design of gastroretentive microsponges for enhanced bioavailability of Dapagliflozin. *Drug Deliv.* **25**, 1400–1410. https://doi.org/10.1080/10717544.2018.1474963 (2018).
42. Attimarad, M., Harsha, N. S. & Nair, A. B. HPLC–UV method for determination of dapagliflozin: application to rat pharmacokinetics. *J. Liq. Chromatogr. Relat. Technol.* **42**, 97–103. https://doi.org/10.1080/10826076.2019.1580609 (2019).
43. European Medicines, A. *Guideline on Bioanalytical Method Validation* (EMA, 2011).
44. Food, U. S. & Drug, A. *Bioanalytical Method Validation Guidance for Industry* (FDA, 2018).
45. Nirogi, R. et al. Bioanalytical method validation for small molecules: A scientific approach. *Bioanalysis* **6**, 2691–2707. https://doi.org/10.4155/bio.14.197 (2014).
46. Chettupalli, A. K., Hagbani, A., Khalid, M. & T. & Development of Dapagliflozin solid lipid nanoparticles as a novel carrier for oral delivery. *Pharmaceuticals* **15**, 568. https://doi.org/10.3390/ph15050568 (2022).
47. Sharma, J. B., Tiwari, A. & Kumar, M. Statistical optimization of Tetrahydrocurcumin loaded solid lipid nanoparticles using box Behnken design. *Saudi Pharm. J.* **31**, 1230–1242. https://doi.org/10.1016/j.jsps.2023.02.003 (2023).
48. Göçmez, S. S., Mert, S. & Çelebi, G. in *Nanotechnology Ind. Biomedicine* 166–175 (2021).
49. Unnisa, A., Chettupalli, A. K. & Al Hagbani, T. Development and optimization of Dapagliflozin oral nano-bilosomes using response surface methodology. *Pharmaceuticals* **15**, 710 (2022).
50. Al-Hashimi, N., Babenko, M. & Saaed, M. The impact of natural and synthetic polymers in formulating micro and nanoparticles for anti-diabetic drugs. *Curr. Drug Deliv.* **18**, 263–275. https://doi.org/10.2174/1567201817999201202201746 (2021).
51. Kazi, M., Alqahtani, A. & Ahmad, A. Development and optimization of sitagliptin and Dapagliflozin loaded oral self-nanoemulsifying formulation against type 2 diabetes mellitus. *Drug Deliv.* **28**, 1761–1775. https://doi.org/10.1080/10717544.2020.1859001 (2021).
52. Al-Hashimi, N. Nanoparticle formulation of poorly soluble drugs: effect on bioavailability and surface properties. *Eur. J. Pharm. Sci.* **155**, 105553. https://doi.org/10.1016/j.ejps.2020.105553 (2020).
53. Yuan, Y. Alginate–PVA nanoparticles for oral drug delivery. *Int. J. Biol. Macromol.* **92**, 539–546. https://doi.org/10.1016/j.ijbiomac.2016.07.021 (2016).
54. Ahmed, F., Ali, S. & Khan, S. Polymer-based nanoparticles for improved cellular uptake and drug retention in cancer therapy. *J. Nanobiotechnol.* **19**, 234. https://doi.org/10.1186/s12951-021-00952-3 (2021).
55. Zhang, Y., Zhao, L. & Wang, H. Enhanced anticancer efficacy of nanoformulated Dapagliflozin in gastric cancer cells. *Int. J. Pharm.* **610**, 121221. https://doi.org/10.1016/j.ijpharm.2021.121221 (2022).
56. Zhang, L. A. U. Z. X. A. U. H. Y. Advances in the development of nanocarriers for enhancing oral bioavailability of poorly soluble drugs. *Asian J. Pharm. Sci.* **15**, 191–210 (2020).
57. Patel, D. Development and characterization of Colon-Targeted nanoparticles. *Mater. Sci. Engineering: C.* **120**, 111701. https://doi.org/10.1016/j.msec.2020.111701 (2021).
58. Dash, S. A. & U. M. P. N. A. U. N. L. A. U. C. P. Kinetic modeling on drug release from controlled drug delivery systems. *Acta Pol. Pharm.* **67**, 217–223 (2010).
59. Sato, Y. & Ishii, M. Gastro-retentive drug delivery using alginate-based gel systems. *Carbohydr. Polym.* **195**, 156. https://doi.org/10.1016/j.carbpol.2018.04.077 (2018). 164-156–164.
60. Singh, R., Bharti, N. & Madan, J. Evaluation of polymeric nanoparticles in cancer therapy: mucoadhesive and permeability properties. *Eur. J. Pharm. Biopharm.* **156**, 45–55. https://doi.org/10.1016/j.ejpb.2020.08.010 (2020).
61. Chen, J. & Wang, Y. Polyvinyl alcohol: A review of its structure, properties and applications. *Mater. Today*. **42**, 125 (2020).
62. Ahmed, M. & Li, C. Dapagliflozin nanocarriers inhibit tumor growth through MAPK/ERK pathway modulation. *Cancer Nanotechnol.* **14**, 17 (2023).
63. Wei, Y. & Dong, Y. TGF-beta signaling Inhibition in cancer therapy. *Cancer Res.* **81**, 3892 (2021).
64. Gupta, R. A. U. B., A. A. & U. D. S. Molecular insights into inflammation and cancer: bridging pathways through therapeutic interventions. *Cancer Lett.* **509**, 30–43 (2021).
65. El-Say, K. M. Polymer-based nanocarriers for oral delivery of antidiabetic drugs: mechanisms and clinical implications. *Drug Deliv.* **27**, 1080–1093. https://doi.org/10.1080/10717544.2020.1762022 (2020).
66. Patel, D. J. A. & U. A. Y. K. A. U. R. A. P. Recent advances in gastroretentive drug delivery systems: A review. *Drug Dev. Ind. Pharm.* **42**, 527–538 (2016).
67. Li, X., Wang, Y. & Luo, Y. Mucoadhesive nanocarriers for oral drug delivery: A review. *Carbohydr. Polym.* **199**, 1–11. https://doi.org/10.1016/j.carbpol.2018.06.084 (2018).
68. Zhao, H. & Tang, H. Biodegradable polymeric nanoparticles in cancer therapy. *Acta Biomater.* **122**, 1 (2021).
69. Kumar, V. & Singh, A. Improved oral bioavailability of poorly soluble drugs through nanoparticle systems. *Int. J. Pharm.* **613**, 121316 (2022).

Acknowledgements

This work was funded by two grants from the Deanship of Scientific Research and Graduate Studies, Applied Science Private University, Amman, Jordan (DRGS/2024/11), and Princess Nourah bint Abdulrahman University Researchers Supporting Project Number (PNURSP2026R305), Princess Nourah bint Abdulrahman University, Riyadh, Saudi Arabia.

Author contributions

Samaa Abdullah and Samar Thiab contributed equally to the conception and design of the study, supervised all experimental work, and were primarily responsible for the interpretation of results and critical revision of the manuscript for important intellectual content. Both authors approved the final version of the manuscript and agreed to be accountable for all aspects of the work.Alaa A. Al-Masud and Abeer A. Altamimi have contributed to the drafting of the results and discussion sections.Sara Faludah and Ahmed Saud Abdulhameed have contributed to analytical method development and pharmacokinetic modelling and assisted in the validation and visualization of data.

Funding
This work was funded by two grants from the Deanship of Scientific Research and Graduate Studies, Applied Science Private University, Amman, Jordan (DRGS/2024/11), and Princess Nourah bint Abdulrahman University Researchers Supporting Project Number (PNURSP2026R305), Princess Nourah bint Abdulrahman University, Riyadh, Saudi Arabia.

Declarations

Competing interests
The authors declare no competing interests.

Consent for publication
All authors have reviewed the final manuscript and consent to its submission and publication.

Additional information
Supplementary Information The online version contains supplementary material available at https://doi.org/10.1038/s41598-026-36232-8.

Correspondence and requests for materials should be addressed to S.A.

Reprints and permissions information is available at www.nature.com/reprints.

Publisher's note Springer Nature remains neutral with regard to jurisdictional claims in published maps and institutional affiliations.